Journal of Computational Physics 421 (2020) 109733

Contents lists available at ScienceDirect

Journal of Computational Physics

www.elsevier.com/locate/jcp

A Jacobi spectral method for computing eigenvalue gaps and their distribution statistics of the fractional Schrödinger operator

Weizhu Bao [a], Lizhen Chen [b,a,*], Xiaoyun Jiang [c], Ying Ma [b]

[a] Department of Mathematics, National University of Singapore, Singapore 119076, Singapore
[b] Beijing Computational Science Research Center, Beijing, 100193, PR China
[c] School of Mathematics, Shandong University, Jinan 250100, PR China

ARTICLE INFO

Article history:
Received 10 April 2020
Received in revised form 18 July 2020
Accepted 20 July 2020
Available online 3 August 2020

Keywords:
Fractional Schrödinger operator
Jacobi spectral method
Nearest neighbour gaps
Minimum gaps
Normalized gaps
Gaps distribution statistics

ABSTRACT

We propose a spectral method by using the Jacobi functions for computing eigenvalue gaps and their distribution statistics of the fractional Schrödinger operator (FSO). In the problem, in order to get reliable gaps distribution statistics, we have to calculate accurately and efficiently a very large number of eigenvalues, e.g. up to thousands or even millions eigenvalues, of an eigenvalue problem related to the FSO. For simplicity, we start with the eigenvalue problem of the FSO in one dimension (1D), reformulate it into a variational formulation and then discretize it by using the Jacobi spectral method. Our numerical results demonstrate that the proposed Jacobi spectral method has several advantages over the existing finite difference method (FDM) and finite element method (FEM) for the problem: (i) the Jacobi spectral method is spectral accurate, while the FDM and FEM are only first order accurate; and more importantly (ii) under a fixed number of degree of freedoms M, the Jacobi spectral method can calculate accurately a large number of eigenvalues with the number proportional to M, while the FDM and FEM perform badly when a large number of eigenvalues need to be calculated. Thus the proposed Jacobi spectral method is extremely suitable and demanded for the discretization of an eigenvalue problem when a large number of eigenvalues need to be calculated. Then the Jacobi spectral method is applied to study numerically the asymptotics of the nearest neighbour gaps, average gaps, minimum gaps, normalized gaps and their distribution statistics in 1D. Based on our numerical results, several interesting numerical observations (or conjectures) about eigenvalue gaps and their distribution statistics of the FSO in 1D are formulated. Finally, the Jacobi spectral method is extended to the directional fractional Schrödinger operator in high dimensions and extensive numerical results about eigenvalue gaps and their distribution statistics are reported.

* Corresponding author at: Beijing Computational Science Research Center, Beijing, 100193, PR China.
E-mail addresses: matbaowz@nus.edu.sg (W. Bao), lzchen@csrc.ac.cn (L. Chen), wqjxyf@sdu.edu.cn (X. Jiang), yingma@csrc.ac.cn (Y. Ma).
URL: http://blog.nus.edu.sg/matbwz/ (W. Bao).

https://doi.org/10.1016/j.jcp.2020.109733

1. Introduction

Consider the eigenvalue problem of the fractional Schrödinger operator (FSO) (or time-independent fractional Schrödinger equation in the dimensionless form) in one dimension (1D):

Find $\lambda \in \mathbb{R}$ and a nonzero real-valued function $u(x) \neq 0$ such that

$$\begin{aligned} &L_{\mathrm{FSO}}\, u(x) := \Big[(-\partial_{xx})^{\alpha/2} + V(x)\Big] u(x) = \lambda\, u(x), \qquad x \in \Omega := (a,b), \\ &\quad u(x) = 0, \qquad x \in \Omega^c := \mathbb{R}\backslash\Omega, \end{aligned} \tag{1.1}$$

where $0 < \alpha \le 2$, $V(x) \in L^\infty(\Omega)$ is a given real-valued function and the fractional Laplacian operator (FLO) $(-\partial_{xx})^{\alpha/2}$ is defined via the Fourier transform (see [71,28,42,46] and references therein) as

$$(-\partial_{xx})^{\alpha/2}\, u(x) = \mathcal{F}^{-1}(|\xi|^\alpha (\mathcal{F}u)(\xi)), \qquad x, \xi \in \mathbb{R}, \tag{1.2}$$

with $\mathcal{F}$ and $\mathcal{F}^{-1}$ the Fourier transform and the inverse Fourier transform [19,46,36], respectively. We remark here that an alternative way to define $(-\partial_{xx})^{\alpha/2}$ is through the principle value integral (see [63,65,29,49,28] and references therein) as

$$(-\partial_{xx})^{\alpha/2}\, u(x) := C_1^\alpha \int_{\mathbb{R}} \frac{u(x) - u(y)}{|x-y|^{1+\alpha}} dy, \qquad x \in \mathbb{R}, \tag{1.3}$$

where C_1^α is a constant whose value can be computed explicitly as

$$C_1^\alpha = \frac{2^\alpha \Gamma((1+\alpha)/2)}{\pi^{1/2} |\Gamma(-\alpha/2)|} = \frac{\alpha \Gamma((1+\alpha)/2)}{2^{1-\alpha} \pi^{1/2} \Gamma(1-\alpha/2)}.$$

Another remark here is that the problem (1.1) is equivalent to the problem defined on the whole x-axis $\mathbb{R}$ by taking the potential $V(x) = +\infty$ for $x \in \Omega^c$, while the claim on the equivalence between the two problems is well accepted for the Schrödinger operator, i.e. $\alpha = 2$, and has been numerically verified for $0 < \alpha \le 2$ via the problem defined on the whole x-axis $\mathbb{R}$ by taking a well potential $V(x) = V_0$ for $x \in \Omega^c$ with $V_0 \to +\infty$ (see Section 4.5 in [12]). When $\alpha = 2$, (1.1) collapses to the (classical) time-independent Schrödinger equation (or a standard Sturm-Liouville eigenvalue problem) which has been widely used for determining energy levels and their corresponding stationary states of a quantum particle within an external potential $V(x)$ in quantum physics and chemistry [27] and many other areas [48,23,25]. When $\alpha = 1$, the FLO $(-\Delta)^{1/2}$ and its variation $(\beta - \Delta)^{1/2}$ with $\beta > 0$ a constant have been widely adopted in representing the Coulomb interaction and the dipole-dipole interaction in two dimensions (2D) [8,10,20,40] and modelling the relativistic quantum mechanics for boson star [32,9]. When $0 < \alpha < 2$, (1.1) is usually referred to the time-independent fractional Schrödinger equation (or fractional eigenvalue problem) which has been widely adopted for computing energy levels and their stationary states in fractional quantum mechanics [49,10,20,70,50,3], polariton condensation and quantum fluids of lights [21,57], while the FSO can be interpreted via the Feynman path integral approach over Brownian-like quantum paths or over the Lévy-like quantum paths, see [65,49,41] and references therein.

Without loss of generality, we assume that $V(x)$ is non-negative, i.e. $V(x) \ge 0$ for $x \in \Omega$. Since all eigenvalues of (1.1) are distinct (or all spectrum are discrete and no continuous spectrum) [5], we can rank (or order) all eigenvalues $\{\lambda_n^\alpha \mid n = 1, 2, \ldots\}$ (with the superscript α referring to the fractional exponent instead of a power) of (1.1) as

$$0 < \lambda_1^\alpha < \lambda_2^\alpha \le \ldots \le \lambda_n^\alpha \le \ldots, \tag{1.4}$$

where the times that an eigenvalue λ of (1.1) appears in the above sequence (1.4) is the same as its algebraic multiplicity. When $V(x) \equiv 0$ for $x \in \Omega$, all eigenvalues of (1.1) are simple eigenvalues, i.e. their algebraic multiplicities are all equal to 1, then all $\le$ in (1.4) can be replaced by $<$. Define the *nearest neighbour gaps* as [39]

$$\delta_{\mathrm{nn}}^\alpha(N) := \lambda_{N+1}^\alpha - \lambda_N^\alpha, \qquad N = 1, 2, 3, \ldots, \tag{1.5}$$

where when $N = 1$, i.e., $\delta_{\mathrm{nn}}^\alpha(1) = \lambda_2^\alpha - \lambda_1^\alpha := \delta_{\mathrm{fg}}(\alpha)$ (i.e. the difference between the first two smallest eigenvalues) is called as the *fundamental gap* of the FSO (1.1), which has been studied analytically and/or numerically for $\alpha = 2$ [4,1,11,13] and $0 < \alpha \le 2$ [12,16]; the *minimum gaps* as [18,61]

$$\delta_{\min}^\alpha(N) := \min_{1 \le n \le N} \delta_{\mathrm{nn}}^\alpha(n) = \min_{1 \le n \le N} \lambda_{n+1}^\alpha - \lambda_n^\alpha, \qquad N = 1, 2, 3, \ldots; \tag{1.6}$$

the *average gaps* as [39]

$$\delta_{\mathrm{ave}}^\alpha(N) := \frac{1}{N} \sum_{n=1}^N \delta_{\mathrm{nn}}^\alpha(n) = \frac{1}{N} \sum_{n=1}^N \left(\lambda_{n+1}^\alpha - \lambda_n^\alpha\right) = \frac{\lambda_{N+1}^\alpha - \lambda_1^\alpha}{N}, \qquad N = 1, 2, \cdots. \tag{1.7}$$

In addition, if there exist two constants $\gamma > 0$ and $C > 0$ such that

$$\lim_{n\to+\infty} \frac{\lambda_n^\alpha}{n^\gamma} = C > 0, \tag{1.8}$$

then the *normalized gaps* (or "unfolding" local statistics in the physics literature) are defined as [39,62]

$$\delta_{\text{norm}}^\alpha(N) := y_{N+1}^\alpha - y_N^\alpha, \qquad N = 1, 2, \dots , \tag{1.9}$$

where

$$y_n^\alpha := \left(\frac{\lambda_n^\alpha}{C}\right)^{1/\gamma}, \qquad n = 1, 2, \dots . \tag{1.10}$$

Then an interesting question is to study their asymptotics, i.e. the behaviour of $\delta_{\text{nn}}^\alpha(N)$, $\delta_{\text{min}}^\alpha(N)$, $\delta_{\text{ave}}^\alpha(N)$ and $\delta_{\text{nrom}}^\alpha(N)$ when $N \to +\infty$, and another interesting and very challenging question is to study the level spacing distribution $P_\alpha(s) :=$ limiting distribution of the normalized gaps $\delta_{\text{norm}}^\alpha(N)$, which is defined as [39,62]

$$\frac{\#\left\{1 \le n \le N \mid \delta_{\text{norm}}^\alpha(n) < x\right\}}{N} \quad \overset{N\to+\infty}{\longrightarrow} \quad \int_0^x P_\alpha(s)ds, \qquad 0 \le x < +\infty, \tag{1.11}$$

where $\#S$ denotes the number of elements in the set S.

When $\alpha = 2$ and $V(x) \equiv 0$ in (1.1), it collapses to a standard Sturm-Liouville eigenvalue problem of the Laplacian operator as

$$\begin{aligned} &L_{\text{SO}}\, u(x) := -\partial_{xx} u(x) = -u''(x) = \lambda\, u(x), \qquad x \in \Omega = (a, b), \\ &\quad u(a) = u(b) = 0. \end{aligned} \tag{1.12}$$

The eigenvalues and their corresponding eigenfunctions of (1.12) can be obtained analytically via the sine series as

$$\lambda_n^{\alpha=2} = \left(\frac{n\pi}{b-a}\right)^2, \qquad u_n(x) = \sin\left(\frac{n\pi(x-a)}{b-a}\right), \qquad n = 1, 2, \dots . \tag{1.13}$$

These results immediately imply that the fundamental gap $\delta_{\text{fg}}(\alpha = 2) = \frac{3\pi^2}{(b-a)^2}$ and

$$\begin{aligned} &\delta_{\text{nn}}^{\alpha=2}(N) = \left(\frac{(N+1)\pi}{b-a}\right)^2 - \left(\frac{N\pi}{b-a}\right)^2 = \frac{\pi^2}{(b-a)^2}(2N+1), \\ &\delta_{\text{min}}^{\alpha=2}(N) \equiv \delta_{\text{nn}}^{\alpha=2}(N=1) = \frac{3\pi^2}{(b-a)^2}, \qquad\qquad\qquad\qquad N = 1, 2, \dots ; \\ &\delta_{\text{ave}}^{\alpha=2}(N) = \frac{1}{N}\left[\left(\frac{(N+1)\pi}{b-a}\right)^2 - \left(\frac{\pi}{b-a}\right)^2\right] = \frac{\pi^2}{(b-a)^2}(N+2), \\ &\delta_{\text{norm}}^{\alpha=2}(N) = y_{N+1}^{\alpha=2} - y_N^{\alpha=2} = N + 1 - N \equiv 1, \end{aligned} \tag{1.14}$$

where

$$y_n^{\alpha=2} = \sqrt{\lambda_n^{\alpha=2} / \left(\frac{\pi}{b-a}\right)^2} = \sqrt{n^2} = n, \qquad n = 1, 2, \dots .$$

From the last equation in (1.14), one can immediately obtain the level spacing distribution defined in (1.11) for $\alpha = 2$ as

$$P_{\alpha=2}(s) = \delta(s-1), \qquad s \ge 0, \tag{1.15}$$

where $\delta(\cdot)$ is the Dirac delta function.

When $\alpha = 2$ and $V(x) \not\equiv 0$ in (1.1), it collapses to a standard Sturm-Liouville eigenvalue problem, which has been extensively studied in the literature. For analytical results, we refer to [44,48,38] and references therein. For numerical methods and results, we refer to [15,6,66] and references therein.

When $0 < \alpha < 2$, in general, one cannot find the eigenvalues of the eigenvalue problem (1.1) analytically and/or explicitly. For mathematical theories of the eigenvalue problem (1.1), we refer to [31,43] and references therein. Some numerical methods have been proposed to solve (1.1) numerically, including an asymptotic method was proposed in [71], a finite element method (FEM) [17] with piecewise linear element was presented in [41] and a finite difference method (FDM) was studied in [30]. The FDM and FEM are usually first order accurate when $0 < \alpha < 2$ and they can be adapted to compute the first several eigenvalues [41,30,17]. However, if we want to calculate accurately and efficiently a very large number of eigenvalues, e.g. up to thousands or even millions eigenvalues, of the eigenvalue problem (1.1) in order to obtain a reliable gaps distribution statistics, the FDM and FEM have severe drawbacks. The main aim of this paper is to propose a spectral method by using the generalized Jacobi functions for computing different eigenvalue gaps and their distribution statistics of the fractional eigenvalue problem related to the FSO (1.1). The proposed numerical method has at least two advantages: (i) it is spectral accurate, and more importantly (ii) under a fixed number of degree of freedoms (DOF) M, it can calculate accurately a large number of eigenvalues with the number proportional to M. Thus this method is a very good candidate for solving our problem, i.e. to compute eigenvalue gaps and their distribution statistics of the fractional eigenvalue problem (1.1).

Based on our extensive numerical results and observations, we speculate the following:

Conjecture (Gaps and their distribution statistics of the FSO in (1.1) without potential) Assume $0 < \alpha < 2$ and $V(x) \equiv 0$ in (1.1), then we have the following asymptotics of its eigenvalues:

$$\lambda_n^\alpha = \left(\frac{n\pi}{b-a}\right)^\alpha - \left(\frac{\pi}{b-a}\right)^\alpha \frac{\alpha(2-\alpha)}{4} n^{\alpha-1} + O(n^{\alpha-2}) = \lambda_{\rm loc}^\alpha(n)\left[1 - \frac{\alpha(2-\alpha)}{4n} + O(n^{-2})\right], \ n \geq 1, \tag{1.16}$$

where $\lambda_{\rm loc}^\alpha(n) = \left(\frac{n\pi}{b-a}\right)^\alpha$ $(n = 1, 2, \dots)$ are the eigenvalues of the *local fractional Laplacian operator* on $\Omega = (a, b)$ with homogeneous Dirichlet boundary condition. Here the local fractional Laplacian denoted as $A^{\alpha/2}$ is defined via the spectral decomposition of the Laplacian operator [12]: For a bounded domain $\Omega \subset \mathbb{R}$, let λ_m and u_m $(m \in \mathbb{N})$ be the eigenvalues and their corresponding eigenfunctions of the Laplacian operator $-\Delta$ on Ω with the homogeneous Dirichlet boundary condition, then for any $\alpha \in (0, 2)$ and $\phi(x) \in H_0^1(\Omega)$ with $\phi(x) = \sum_{m\in\mathbb{N}} a_m u_m(x)$ for $x \in \overline{\Omega}$, we define the operator $A^{\alpha/2}$ in the following way $A^{\alpha/2}\phi(x) = \sum_{m\in\mathbb{N}} a_m (\lambda_m)^{\alpha/2} u_m(x)$ for $x \in \overline{\Omega}$.

From (1.16), we obtain immediately the following approximations of different gaps:

$$\begin{aligned}
&\delta_{\rm nn}^\alpha(N) \approx \left(\frac{\pi}{b-a}\right)^\alpha \left[\alpha N^{\alpha-1} + \frac{\alpha(\alpha-1)(2+\alpha)}{4} N^{\alpha-2} + O(N^{\alpha-3})\right], \quad 0 < \alpha < 2, \\
&\delta_{\min}^\alpha(N) = \begin{cases} \delta_{\rm nn}^\alpha(1) = \lambda_2^\alpha - \lambda_1^\alpha, & 1 < \alpha < 2, \\ \approx \delta_{\rm nn}^\alpha(1) = \lambda_2^\alpha - \lambda_1^\alpha, & \alpha = 1, \\ \delta_{\rm nn}^\alpha(N) = \lambda_{N+1}^\alpha - \lambda_N^\alpha \approx \alpha\left(\frac{\pi}{b-a}\right)^\alpha N^{\alpha-1}, & 0 < \alpha < 1, \end{cases} \\
&\delta_{\rm ave}^\alpha(N) \approx \left(\frac{\pi}{b-a}\right)^\alpha \begin{cases} \left[N^{\alpha-1} + \frac{\alpha(2+\alpha)}{4} N^{\alpha-2} + O(N^{-1})\right], & 1 < \alpha < 2, \\ \left[1 + \left(\frac{3}{4} - \frac{b-a}{\pi}\lambda_1^{\alpha=1}\right) N^{-1} + O(N^{-2})\right], & \alpha = 1, \\ \left[N^{\alpha-1} - \left(\frac{b-a}{\pi}\right)^\alpha \lambda_1^\alpha N^{-1} + O(N^{\alpha-2})\right], & 0 < \alpha < 1, \end{cases} \\
&\delta_{\rm norm}^\alpha(N) \approx 1 + O(N^{-2}), \qquad 0 < \alpha < 2,
\end{aligned} \qquad N \geq 1. \tag{1.17}$$

In addition, for the gaps distribution statistics defined in (1.11), we have

$$P_\alpha(s) = \delta(s-1), \qquad s \geq 0, \qquad 0 < \alpha \leq 2. \tag{1.18}$$

The paper is organized as follows. In Section 2, we begin with some scaling properties of (1.1) and propose a spectral-Galerkin method by using the generalized Jacobi functions to discretize the fractional eigenvalue problem (1.1). In Section 3, we test the accuracy and resolution capacity (or trust region) with respect to the DOF M of the proposed Jacobi spectral method and compare it with the existing numerical methods such as FDM and FEM. In Section 4, we apply the proposed numerical method to study numerically the asymptotics of different eigenvalue gaps and their distribution statistics of (1.1) without potential and formulate several interesting numerical observations (or conjectures). Similar results are reported in Section 5 for (1.1) with potential. Extensions of the numerical method and results to the directional fractional Schrödinger operator in high dimensions are presented in Section 6. Finally, some conclusions are drawn in Section 7.

2. A Jacobi spectral method

In this section, we begin with a re-scaling argument to the problem (1.1) so as to reduce it on a standard interval $(-1, 1)$, then reformulate it into a variational formulation and discretize the problem by using the Jacobi spectral method.

2.1. Re-scaling property

Introduce

$$x_0=\frac{a+b}{2},\quad L=\frac{b-a}{2},\quad \tilde{x}=\frac{x-x_0}{L},\quad \tilde{V}(\tilde{x})=L^{\alpha}V(x),\quad \tilde{u}(\tilde{x})=u(x_0+L\tilde{x}),\quad x\in\Omega=(a,b), \tag{2.1}$$

and consider the re-scaled fractional eigenvalue problem:

Find $\tilde{\lambda}\in\mathbb{R}$ and a real-valued function $\tilde{u}(\tilde{x})\neq 0$ such that

$$\begin{aligned}&\tilde{L}_{\mathrm{FSO}}\,\tilde{u}(\tilde{x}):=\left[(-\partial_{\tilde{x}\tilde{x}})^{\alpha/2}+\tilde{V}(\tilde{x})\right]\tilde{u}(\tilde{x})=\tilde{\lambda}\,\tilde{u}(\tilde{x}),\qquad \tilde{x}\in\tilde{\Omega}:=(-1,1),\\ &\quad\tilde{u}(\tilde{x})=0,\qquad \tilde{x}\in\tilde{\Omega}^c:=\mathbb{R}\backslash\tilde{\Omega};\end{aligned} \tag{2.2}$$

then we have

Lemma 2.1. *Let $\tilde{\lambda}$ be an eigenvalue of (2.2) and $\tilde{u}:=\tilde{u}(\tilde{x})$ be the corresponding eigenfunction, then $\lambda=L^{-\alpha}\tilde{\lambda}$ is an eigenvalue of (1.1) and $u:=u(x)=\tilde{u}(\tilde{x})=\tilde{u}\left(\frac{x-x_0}{L}\right)$ is the corresponding eigenfunction. Assume that $0<\tilde{\lambda}_1^{\alpha}<\tilde{\lambda}_2^{\alpha}\le\ldots\le\tilde{\lambda}_n^{\alpha}\le\ldots$ are all eigenvalues of (2.2), then $0<\lambda_1^{\alpha}<\lambda_2^{\alpha}\le\ldots\le\lambda_n^{\alpha}\le\ldots$ (ranked as in (1.4)) with $\lambda_n^{\alpha}=L^{-\alpha}\tilde{\lambda}_n^{\alpha}$ $(n=1,2,\ldots)$ are all eigenvalues of (1.1). In addition, we have the scaling property on the different gaps as*

$$\begin{aligned}&\delta_{\mathrm{nn}}^{\alpha}(N)=L^{-\alpha}\tilde{\delta}_{\mathrm{nn}}^{\alpha}(N),\qquad \textit{with}\quad \tilde{\delta}_{\mathrm{nn}}^{\alpha}(N):=\tilde{\lambda}_{N+1}^{\alpha}-\tilde{\lambda}_N^{\alpha},\\ &\delta_{\min}^{\alpha}(N)=L^{-\alpha}\tilde{\delta}_{\min}^{\alpha}(N),\qquad \textit{with}\quad \tilde{\delta}_{\min}^{\alpha}(N):=\min_{1\le n\le N}\tilde{\delta}_{\mathrm{nn}}^{\alpha}(n),\\ &\delta_{\mathrm{ave}}^{\alpha}(N)=L^{-\alpha}\tilde{\delta}_{\mathrm{ave}}^{\alpha}(N),\qquad \textit{with}\quad \tilde{\delta}_{\mathrm{ave}}^{\alpha}(N):=\frac{1}{N}\sum_{n=1}^{N}\tilde{\delta}_{\mathrm{nn}}^{\alpha}(n),\qquad N=1,2,\ldots;\\ &\delta_{\mathrm{norm}}^{\alpha}(N)=\tilde{\delta}_{\mathrm{norm}}^{\alpha}(N),\qquad \textit{with}\quad \tilde{\delta}_{\mathrm{norm}}^{\alpha}(N):=\tilde{y}_{N+1}^{\alpha}-\tilde{y}_N^{\alpha},\quad \tilde{y}_N^{\alpha}=\left(\frac{\tilde{\lambda}_N^{\alpha}}{L^{\alpha}C}\right)^{1/\gamma},\end{aligned} \tag{2.3}$$

which immediately imply that the level spacing distribution $P_{\alpha}(s)$ of (1.1) does not change under the re-scaling (2.1), i.e. the problems (1.1) and (2.2) have the same level spacing distribution.

Proof. From (1.3) and noticing (2.1), a direct computation implies the re-scaling property of the fractional Laplacian operator

$$\begin{aligned}(-\partial_{xx})^{\alpha/2}u(x)&=C_1^{\alpha}\int_{\mathbb{R}}\frac{u(x)-u(y)}{|x-y|^{1+\alpha}}\,dy=C_1^{\alpha}\int_{\mathbb{R}}\frac{u(x_0+L\tilde{x})-u(x_0+L\tilde{y})}{|x_0+L\tilde{x}-x_0-L\tilde{y}|^{1+\alpha}}\,L\,d\tilde{y}\\ &=L^{-\alpha}C_1^{\alpha}\int_{\mathbb{R}}\frac{\tilde{u}(\tilde{x})-\tilde{u}(\tilde{y})}{|\tilde{x}-\tilde{y}|^{1+\alpha}}\,d\tilde{y}=L^{-\alpha}\,(-\partial_{\tilde{x}\tilde{x}})^{\alpha/2}\,\tilde{u}(\tilde{x}),\quad x\in\Omega,\quad \tilde{x}\in\tilde{\Omega}.\end{aligned} \tag{2.4}$$

Noticing

$$u(x)=0,\quad x\in\Omega^c\qquad\Longleftrightarrow\qquad \tilde{u}(\tilde{x})=0,\quad \tilde{x}\in\tilde{\Omega}^c. \tag{2.5}$$

Substituting (2.4) into (2.2), noting (1.1), we get

$$\begin{aligned}\tilde{\lambda}\,u(x)&=\tilde{\lambda}\,\tilde{u}(\tilde{x})=\left[(-\partial_{\tilde{x}\tilde{x}})^{\frac{\alpha}{2}}+\tilde{V}(\tilde{x})\right]\tilde{u}(\tilde{x})=\left[L^{\alpha}\,(-\partial_{xx})^{\frac{\alpha}{2}}+\tilde{V}\left(\frac{x-x_0}{L}\right)\right]u(x)\\ &=L^{\alpha}\left[(-\partial_{xx})^{\frac{\alpha}{2}}+L^{-\alpha}\tilde{V}\left(\frac{x-x_0}{L}\right)\right]u(x)\\ &=L^{\alpha}\left[(-\partial_{xx})^{\frac{\alpha}{2}}+V(x)\right]u(x),\qquad x\in\Omega,\quad \tilde{x}\in\tilde{\Omega},\end{aligned} \tag{2.6}$$

which immediately implies that $u(x)$ is an eigenfunction of the operator $(-\partial_{xx})^{\frac{\alpha}{2}}+V(x)$ with the eigenvalue $\lambda=L^{-\alpha}\tilde{\lambda}$.

From the assumption (1.4) with $\Omega=(-1,1)$ that $0<\tilde{\lambda}_1^{\alpha}<\tilde{\lambda}_2^{\alpha}\le\ldots\le\tilde{\lambda}_n^{\alpha}\le\ldots$ are all eigenvalues of (2.2), we get immediately that $0<\lambda_1^{\alpha}<\lambda_2^{\alpha}\le\ldots\le\lambda_n^{\alpha}\le\ldots$ with $\lambda_n^{\alpha}=L^{-\alpha}\tilde{\lambda}_n^{\alpha}$ $(n=1,2,\ldots)$ are all eigenvalues of the eigenvalue problem (1.1). Then the re-scaling property on the different gaps (2.3) can be obtained straightforwardly by using $\tilde{\lambda}_n^{\alpha}=L^{\alpha}\lambda_n^{\alpha}$ $(n=1,2,\ldots)$. $\square$

2.2. A variational formulation

Following those in the literature [45,35], we introduce the fractional functional space $H^{\frac{\alpha}{2}}(\mathbb{R})$ through the Fourier transform

$$H^{\frac{\alpha}{2}}(\mathbb{R}) = \left\{ v \in \mathcal{D}'(\mathbb{R}) \mid \|v\|_{\frac{\alpha}{2},\mathbb{R}} < \infty \right\}, \tag{2.7}$$

where the norms are defined as

$$|v|_{\frac{\alpha}{2},\mathbb{R}} = \left(\int_{\mathbb{R}} |\xi|^{\alpha} \, |(\mathcal{F}v)(\xi)|^2 \, d\xi \right)^{\frac{1}{2}}, \qquad \|v\|_{\frac{\alpha}{2},\mathbb{R}} = \left(\int_{\mathbb{R}} (1+|\xi|^2)^{\frac{\alpha}{2}} \, |(\mathcal{F}v)(\xi)|^2 \, d\xi \right)^{\frac{1}{2}}; \tag{2.8}$$

and then the fractional functional space $H^{\frac{\alpha}{2}}(\Omega)$ can be obtained from $H^{\frac{\alpha}{2}}(\mathbb{R})$ by extension [45,35]

$$H^{\frac{\alpha}{2}}(\Omega) = \left\{ v : \Omega \to \mathbb{R} \mid \hat{v} = E_{\Omega} v \in H^{\frac{\alpha}{2}}(\mathbb{R}) \right\}, \tag{2.9}$$

where the norms are defined as

$$|v|_{\frac{\alpha}{2}} := |v|_{\frac{\alpha}{2},\Omega} = |E_{\Omega} v|_{\frac{\alpha}{2},\mathbb{R}}, \qquad \|v\|_{\frac{\alpha}{2}} := \|v\|_{\frac{\alpha}{2},\Omega} = \|E_{\Omega} v\|_{\frac{\alpha}{2},\mathbb{R}}, \qquad \forall v \in H^{\frac{\alpha}{2}}(\Omega), \tag{2.10}$$

with $\hat{v} = E_{\Omega} v : \mathbb{R} \to \mathbb{R}$ (extension of v from Ω to $\mathbb{R}$) defined as

$$\hat{v}(x) = (E_{\Omega} v)(x) = \begin{cases} v(x), & x \in \Omega, \\ 0, & x \in \mathbb{R} \backslash \Omega. \end{cases} \tag{2.11}$$

For any $v \in H^{\frac{\alpha}{2}}(\Omega)$, multiplying v to (1.1) and integrating over Ω and using integration by parts, we obtain the variational (or weak) formulation of the fractional eigenvalue problem (1.1) as:

find $\lambda \in \mathbb{R}$ and $0 \neq u \in H^{\frac{\alpha}{2}}(\Omega)$ such that

$$a(u, v) = \lambda \, b(u, v), \qquad \forall v \in H^{\frac{\alpha}{2}}(\Omega), \tag{2.12}$$

where the bilinear forms $a(\cdot, \cdot)$ and $b(\cdot, \cdot)$ are given as

$$\begin{aligned} a(u, v) &= \int_{\Omega} \left[(-\partial_{xx})^{\frac{\alpha}{2}} u + V(x) u \right] v dx = \int_{\Omega} \left[(-\partial_{xx})^{\frac{\alpha}{4}} u \, (-\partial_{xx})^{\frac{\alpha}{4}} v + V(x) u v \right] dx, \\ b(u, v) &= \int_{\Omega} u(x) v(x) dx, \qquad \forall u, v \in H^{\frac{\alpha}{2}}(\Omega). \end{aligned} \tag{2.13}$$

2.3. A spectral discretization by using the Jacobi functions

Since we are mainly interested in gaps and their distribution statistics, from the results in Lemma 2.1, without loss of generality, from now on, we always assume that $\Omega = (-1, 1)$, i.e. $a = -1$ and $b = 1$ in (1.1).

Let $\{P_n^{\frac{\alpha}{2},\frac{\alpha}{2}}(x)\}_{n=0}^{\infty}$ denote the classical Jacobi polynomials (or Gegenbauer polynomials) which are orthogonal with respect to the weight function $\omega^{\frac{\alpha}{2},\frac{\alpha}{2}}(x) = (1-x^2)^{\frac{\alpha}{2}}$ over the interval $(-1, 1)$, i.e.

$$\int_{-1}^{1} P_n^{\frac{\alpha}{2},\frac{\alpha}{2}}(x) \, P_m^{\frac{\alpha}{2},\frac{\alpha}{2}}(x) \, \omega^{\frac{\alpha}{2},\frac{\alpha}{2}}(x) dx = C_n \delta_{nm}, \qquad n, m = 0, 1, 2, \ldots, \tag{2.14}$$

where δ_{nm} is the Kronecker delta and

$$C_n = \frac{2^{\alpha+1}}{2n+\alpha+1} \frac{\Gamma(n+\alpha/2+1)^2}{\Gamma(n+\alpha+1) n!} \qquad n = 0, 1, 2 \ldots . \tag{2.15}$$

Based on the boundary behaviour of the solutions of the FLO [36,37,51] and easy to evaluate the Galerkin matrices, we define the generalized Jacobi functions

$$\mathcal{J}_n^{-\frac{\alpha}{2},-\frac{\alpha}{2}}(x) = (1-x^2)^{\frac{\alpha}{2}} P_n^{\frac{\alpha}{2},\frac{\alpha}{2}}(x) = \omega^{\frac{\alpha}{2},\frac{\alpha}{2}}(x) \, P_n^{\frac{\alpha}{2},\frac{\alpha}{2}}(x), \quad -1 \leq x \leq 1, \qquad n = 0, 1, 2, \ldots . \tag{2.16}$$

Then by Theorem 2 in Ref. [51], we have

$$(-\partial_{xx})^{\frac{\alpha}{2}} \mathcal{J}_n^{-\frac{\alpha}{2},-\frac{\alpha}{2}}(x) = \frac{\Gamma(n+\alpha+1)}{n!} P_n^{\frac{\alpha}{2},\frac{\alpha}{2}}(x), \quad -1 < x < 1, \qquad n = 0, 1, 2, \dots . \tag{2.17}$$

Combining (2.16) and (2.17), we obtain

$$\begin{aligned}
&\int_{-1}^{1} (-\partial_{xx})^{\frac{\alpha}{2}} \mathcal{J}_n^{-\frac{\alpha}{2},-\frac{\alpha}{2}}(x)\, \mathcal{J}_m^{-\frac{\alpha}{2},-\frac{\alpha}{2}}(x)\, dx = \int_{-1}^{1} \mathcal{J}_n^{-\frac{\alpha}{2},-\frac{\alpha}{2}}(x)\, (-\partial_{xx})^{\frac{\alpha}{2}} \mathcal{J}_m^{-\frac{\alpha}{2},-\frac{\alpha}{2}}(x)\, dx \\
&= \int_{-1}^{1} (-\partial_{xx})^{\frac{\alpha}{4}} \mathcal{J}_n^{-\frac{\alpha}{2},-\frac{\alpha}{2}}(x)\, (-\partial_{xx})^{\frac{\alpha}{4}} \mathcal{J}_m^{-\frac{\alpha}{2},-\frac{\alpha}{2}}(x)\, dx = \int_{-1}^{1} \frac{\Gamma(n+\alpha+1)}{n!} P_n^{\frac{\alpha}{2},\frac{\alpha}{2}}(x)\, \mathcal{J}_m^{-\frac{\alpha}{2},-\frac{\alpha}{2}}(x)\, dx \\
&= \frac{\Gamma(n+\alpha+1)}{n!} \int_{-1}^{1} P_n^{\frac{\alpha}{2},\frac{\alpha}{2}}(x)\, P_m^{\frac{\alpha}{2},\frac{\alpha}{2}}(x)\, \omega^{\frac{\alpha}{2},\frac{\alpha}{2}}(x)\, dx \\
&= \frac{2^{\alpha+1}\Gamma(n+\alpha/2+1)^2}{(n!)^2(2n+\alpha+1)} \delta_{nm}, \quad n, m = 0, 1, 2 \dots .
\end{aligned} \tag{2.18}$$

Introduce

$$\phi_n(x) := \frac{\sqrt{2n+\alpha+1}\,n!}{2^{\alpha/2+1/2}\Gamma(n+\alpha/2+1)} \mathcal{J}_n^{-\frac{\alpha}{2},-\frac{\alpha}{2}}(x), \quad -1 \le x \le 1, \qquad n = 0, 1, 2, \dots . \tag{2.19}$$

Let $M > 0$ be a positive integer and define the finite dimensional space (which is an approximate subspace of $H^{\frac{\alpha}{2}}(\Omega)$) as

$$\mathbb{W}_M := \operatorname{span}\{\phi_m(x),\ 0 \le m \le M-1\}, \tag{2.20}$$

then a Jacobi spectral method (JSM) for (2.12) is given as:

Find $\lambda_M \in \mathbb{R}$ and $0 \ne u_M \in \mathbb{W}_M$ such that

$$a(u_M, v_M) = \lambda_M\, b(u_M, v_M), \qquad \forall v_M \in \mathbb{W}_M. \tag{2.21}$$

In order to cast the eigenvalue problem (2.21) into the matrix form, we express $u_M \in \mathbb{W}_M$ as a linear combination of the basis functions as

$$u_M(x) = \sum_{m=0}^{M-1} \hat{u}_m\, \phi_m(x), \qquad -1 \le x \le 1. \tag{2.22}$$

Plugging (2.22) into (2.21) and noticing (2.18), after some detailed computation, we obtain the following standard matrix eigenvalue problem:

$$(\mathbf{I}_M + \mathbf{V})\, \hat{U} = \lambda_M\, \mathbf{B}\, \hat{U}, \tag{2.23}$$

where $\hat{U} = (\hat{u}_0, \hat{u}_1, \cdots, \hat{u}_{M-1})^T \in \mathbb{R}^M$ is the eigenvector, $\mathbf{I}_M$ is the $M \times M$ identity matrix, and $\mathbf{V} = (v_{nm})_{0 \le n,m \le M-1} \in \mathbb{R}^{M\times M}$ and $\mathbf{B} = (b_{nm})_{0 \le n,m \le M-1} \in \mathbb{R}^{M\times M}$ are given as

$$\begin{aligned}
v_{nm} &= \int_{-1}^{1} V(x)\phi_n(x)\phi_m(x)dx, \\
& \qquad\qquad\qquad\qquad n, m = 0, 1, \dots, M-1. \\
b_{nm} &= \int_{-1}^{1} \phi_n(x)\phi_m(x)dx,
\end{aligned} \tag{2.24}$$

Plugging (2.19) into the second equation in (2.24), after a detailed computation, we get

$$b_{nm} = \begin{cases} \dfrac{(-1)^{\frac{n-m}{2}} \sqrt{\pi(2n+\alpha+1)(2m+\alpha+1)}\,\Gamma(\alpha+1)(n+m)!}{2^{\alpha+n+m+1}\Gamma(\alpha+\frac{n+m}{2}+\frac{3}{2})\Gamma(\frac{\alpha}{2}+\frac{n-1}{2}+1)\Gamma(\frac{\alpha}{2}+\frac{m-1}{2}+1)(\frac{n+m}{2})!}, & n+m \text{ even}, \\ 0, & n+m \text{ odd}. \end{cases} \tag{2.25}$$

If $V(x) \equiv 0$, then $\mathbf{V} = \mathbf{0}$. Of course, if $V(x) \ne 0$, then the integrals in the first equation in (2.24) can be computed numerically via numerical quadratures with spectral accuracy [59,14,64]. In our practical computations, we adopt the Jacobi-Gauss-Lobatto quadrature (see details on Page 83 of [64]). Finally the matrix eigenvalue problem (2.23) can be solved numerically by the standard eigenvalue solvers such as QR-method [53].

We remark here that different numerical methods have been proposed in the literature for discretizing the fractional Laplacian operator $(-\partial_{xx})^{\alpha/2}$ via the formulation (1.3) or (1.2) or their equivalent forms for numerical simulation of fractional partial differential equations, see [47,69,2,51,56,60,24] and references therein. In fact, a method to discretize the fractional Laplacian operator $(-\partial_{xx})^{\alpha/2}$ can directly generate a method to solve the fractional eigenvalue problem (1.1). For example, a finite element method (FEM) with piecewise linear elements was proposed and analyzed in [41,17] for computing the eigenvalues of (1.1). Similarly, if we adopt the standard finite difference method to discretize the fractional Laplacian operator $(-\partial_{xx})^{\alpha/2}$ [22,47] in (1.1), we can obtain a finite difference method (FDM) for computing the eigenvalues of (1.1). The details are omitted here for brevity.

Due to the singularity of the eigenfunctions of (1.1) (see (4.11) below), only linear convergence rate can be achieved by using FEM or FDM with uniform mesh, even with high order methods, such as the fourth order compact FDM. Thus here we only compare the accuracy and resolution capacity of the proposed Jacobi spectral method with the lowest order FEM or FDM for simplicity. Very recently, the hp-FEM method with adaptive mesh refinement near the boundary was proposed for spectral fractional diffusion [7], which may likely to perform much better than the lowest order FEM or FDM for (1.1).

3. Accuracy and comparison with existing methods

In this section, we test the accuracy and resolution capacity of the Jacobi spectral method (*JSM*) presented in the previous section and compare it with the fractional centred finite difference method (*FDM*) proposed in [69,22] and the finite element method (*FEM*) with piecewise linear elements proposed in [41] for the eigenvalue problem (1.1) with $\Omega = (-1, 1)$. The 'exact' eigenvalues λ_n^α $(n = 1, 2, \dots)$ are obtained numerically by using the JSM (2.21) under a very large DOF $M = M_0$, e.g. $M_0 = 12800$. Let $\lambda_{n,M}^\alpha$ be the numerical approximation of λ_n^α $(n = 1, 2, \dots, M)$ obtained by a numerical method with the DOF chosen as M. Define the absolute and relative errors of λ_n^α as

$$e_n^\alpha := \left|\lambda_n^\alpha - \lambda_{n,M}^\alpha\right|, \qquad e_{n,r}^\alpha := \frac{\left|\lambda_n^\alpha - \lambda_{n,M}^\alpha\right|}{\lambda_n^\alpha}, \qquad n = 1, 2, \dots, \tag{3.1}$$

respectively.

3.1. Accuracy test

We first test convergence rates of different numerical methods for the eigenvalue problem (1.1) including the JSM (2.21), FEM [41,17] and FDM [69,22,30]. Table 1 displays the absolute errors of computing the first eigenvalue of (1.1) with $V(x) \equiv 0$ and different α by using our JSM (2.21), FEM [41] and FDM [69,22]; and Table 2 lists the absolute errors of computing the first, second, fifth and tenth eigenvalues of (1.1) with $\alpha = 0.5$ and $V(x) \equiv 0$ by using those methods. For comparison with the existing results, Table 3 lists the first three eigenvalues of (1.1) with $V(x) \equiv 0$ and different α obtained by using our JSM (2.21) under the DOF $M = 160$ and the asymptotic method in [71] under the DOF $M = 5000$. Fig. 1 shows convergence rates of our JSM (2.21) for computing the first, second, fifth and tenth eigenvalues of (1.1) with $V(x) \equiv 0$ and different α; and Fig. 2 lists similar results of (1.1) with $V(x) = \frac{x^2}{2}$ and different α.

From Tables 1 & 2 and Figs. 1 & 2 and extensive additional results not shown here for brevity, we can draw the following conclusions: (i) For fixed DOF M and $\alpha \in (0, 2]$, the errors from our JSM (2.21) are significantly smaller than those from the FEM [41] and the FDM [69,22] (cf. Tables 1 & 2). (ii) Both the FEM [41] and the FDM [69,22] converge almost quadratically and linearly with respect to the DOF M when $\alpha = 2$ and $0 < \alpha < 2$, respectively (cf. Tables 1 & 2). (iii) Our JSM method (2.21) converges spectrally and sub-spectrally (or super-linearly) with respect to the DOF M when $\alpha = 2$ and $0 < \alpha < 2$, respectively (cf. Fig. 1 & 2). (iv) In Table 3, the numerical results reported by our JSM (2.21) have at least eight significant digits when the DOF $M \geq 160$, while the results by the asymptotic method in [71] have at most four significant digits even when the DOF $M = 5000$. Thus our JSM method (2.21) is significantly accurate than those low-order numerical methods in the literatures for computing eigenvalues of the eigenvalue problem (1.1).

3.2. Resolution capacity (or trust region) test

In order to get reliable gaps and their distribution statistics, we have to calculate accurately and efficiently a very large number of eigenvalues, e.g. up to thousands or even millions eigenvalues. Specifically we need to make sure that the numerical errors are much smaller than the minimum gap of those gaps which are used to find numerically the distribution statistics. In general, to solve the eigenvalue problem (1.1) by a numerical method with a given DOF M, we can obtain M approximate eigenvalues. A key question is that how many eigenvalues or what fraction among the M approximate eigenvalues can be used to find numerically the distribution statistics, i.e. the errors to them are quite small. We remark here that for the Schrödinger operator, i.e. $\alpha = 2$ in (1.1), by using a spectral method, it is proved that about $\frac{2}{\pi}$ fraction of the M approximate eigenvalues are quite accurate (or the errors are quite small) [66]. To see whether this property is still valid for our JSM (2.21) for the FSO (1.1), Fig. 3 displays the relative errors $e_{n,r}^\alpha$ $(n = 1, 2, \dots, 6400)$ of (1.1) with $V(x) \equiv 0$ and different α by using our JSM (2.21), FEM [41] and FDM [69,22] under the DOF $M = 8192$.

Table 1
Absolute errors of computing the first eigenvalue of (1.1) with $\Omega = (-1, 1)$, $V(x) \equiv 0$ and different α by using our JSM (2.21), FEM [41] and FDM [69,22].

		$M=2$	$M=4$	$M=8$	$M=16$	$M=32$	$M=64$	$M=128$	$M=256$
$\alpha=2.0$	JSM	3.63E-5	8.47E-9	1.36E-12	1.36E-12	1.39E-12	1.40E-12	1.17E-12	3.62E-12
	FEM	5.32E-1	1.29E-1	3.18E-2	7.92E-3	1.97E-3	4.87E-4	1.16E-4	2.32E-5
	FDM	4.67E-1	1.24E-1	3.15E-2	7.90E-3	1.97E-3	4.87E-4	1.16E-4	2.32E-5
$\alpha=1.95$	JSM	3.18E-5	1.68E-8	1.78E-11	2.49E-12	2.55E-12	2.24E-12	3.08E-12	2.12E-12
	FEM	4.96E-1	1.16E-2	2.79E-2	6.86E-3	1.72E-3	4.49E-4	1.24E-4	3.78E-5
	FDM	2.31E-1	2.86E-2	5.16E-3	5.41E-4	2.75E-5	7.56E-6	3.76E-6	1.18E-6
$\alpha=1.5$	JSM	2.31E-6	7.17E-7	1.57E-8	1.72E-10	2.16E-12	1.02E-12	6.64E-13	1.41E-12
	FEM	2.72E-1	6.86E-2	2.55E-2	1.18E-2	5.86E-3	2.96E-3	1.49E-3	7.53E-4
	FDM	9.15E-2	6.78E-2	5.41E-2	3.21E-2	1.73E-2	9.01E-3	4.59E-3	2.31E-3
$\alpha=1.0$	JSM	2.16E-5	6.32E-6	3.56E-7	1.15E-8	2.65E-10	4.67E-12	5.94E-13	5.53E-13
	FEM	1.66E-1	5.97E-2	2.29E-2	1.51E-2	7.83E-3	4.01E-3	2.03E-3	1.01E-3
	FDM	1.15E-1	1.00E-1	6.03E-2	3.28E-2	1.71E-2	8.77E-3	4.44E-3	2.24E-3
$\alpha=0.5$	JSM	1.22E-4	3.14E-5	3.95E-6	3.65E-7	2.80E-8	1.94E-9	1.26E-10	7.10E-12
	FEM	8.74E-2	3.93E-2	2.03E-2	1.06E-2	5.54E-3	2.84E-3	1.45E-3	7.35E-4
	FDM	1.08E-1	7.00E-2	3.87E-2	2.04E-2	1.05E-2	5.40E-3	2.74E-3	1.38E-3
$\alpha=0.1$	JSM	1.29E-4	4.01E-5	8.58E-6	1.57E-6	2.68E-7	4.49E-8	7.36E-9	1.06E-9
	FEM	2.02E-2	1.01E-2	5.27E-3	2.75E-3	1.42E-3	7.30E-4	3.72E-4	1.89E-4
	FDM	3.12E-2	1.80E-2	9.59E-3	4.99E-3	2.56E-3	1.31E-3	6.65E-4	3.36E-4

Table 2
Absolute errors of computing the first, second, fifth and tenth eigenvalues of (1.1) with $\Omega = (-1, 1)$, $\alpha = 0.5$ and $V(x) \equiv 0$ by using our JSM (2.21), FEM [41] and FDM [69,22].

		$M=2$	$M=4$	$M=8$	$M=16$	$M=32$	$M=64$	$M=128$	$M=256$
e_1^α	JSM	1.22E-4	3.14E-5	3.95E-6	3.65E-7	2.80E-8	1.94E-9	1.26E-10	7.10E-12
	FEM	8.74E-2	3.93E-2	2.03E-2	1.06E-2	5.54E-3	2.84E-3	1.45E-3	7.35E-4
	FDM	1.08E-1	7.00E-2	3.87E-2	2.04E-2	1.05E-2	5.40E-3	2.74E-3	1.38E-3
e_2^α	JSM	NA	1.88E-4	2.54E-5	2.03E-6	1.41E-7	9.29E-9	5.90E-10	3.42E-11
	FEM	NA	8.03E-2	3.10E-2	1.59E-2	8.49E-3	4.46E-3	2.31E-3	1.18E-3
	FDM	NA	2.54E-2	4.02E-2	2.71E-2	1.55E-2	8.36E-3	4.35E-3	2.23E-3
e_5^α	JSM	NA	NA	2.14E-3	7.30E-6	5.89E-7	4.14E-8	2.73E-9	1.16E-10
	FEM	NA	NA	1.26E-1	3.05E-2	1.33E-2	6.91E-3	3.66E-3	1.91E-3
	FDM	NA	NA	1.19E-2	3.88E-3	1.13E-3	3.10E-4	8.17E-5	2.10E-5
e_{10}^α	JSM	NA	NA	NA	1.02E-2	1.92E-6	1.31E-7	8.44E-9	5.01E-10
	FEM	NA	NA	NA	1.41E-1	2.66E-2	9.96E-3	5.00E-3	2.63E-3
	FDM	NA	NA	NA	2.14E-3	5.99E-4	1.59E-4	4.14E-5	1.06E-5

Table 3
The first three eigenvalues of (1.1) with $\Omega = (-1, 1)$, $V(x) \equiv 0$ and different α obtained numerically by our JSM (2.21) under the DOF $M = 160$ and the asymptotic method in [71] under the DOF $M = 5000$.

	λ_1^α		λ_2^α		λ_3^α	
	JSM (2.21)	Ref. [71]	JSM (2.21)	Ref. [71]	JSM (2.21)	Ref. [71]
$\alpha=1.99$	2.443691434	2.442	9.73318159	9.729	21.82868373	21.829
$\alpha=1.9$	2.244059359	2.243	8.59575252	8.593	18.71689400	18.718
$\alpha=1.8$	2.048734983	2.048	7.50311692	7.501	15.79989416	15.801
$\alpha=1.5$	1.597503545	1.597	5.05975992	5.059	9.59430576	9.957
$\alpha=1.0$	1.157773883	1.158	2.75475474	2.754	4.31680106	4.320
$\alpha=0.5$	0.970165419	0.970	1.60153773	1.601	2.02882105	2.031
$\alpha=0.2$	0.957464477	0.957	1.19653989	1.197	1.31909097	1.320
$\alpha=0.1$	0.972594401	0.973	1.09219649	1.092	1.14732244	1.148
$\alpha=0.01$	0.996634628	0.997	1.00871791	1.009	1.01374130	1.014

From Fig. 3, we can see that our JSM (2.21) is significantly better than the FEM and the FDM when a large number of eigenvalues are to be computed accurately. In fact, the FEM and the FDM can be used to compute the first a few eigenvalues of (1.1). However, when a large amount of eigenvalues are needed, one has to adapt a spectral method such as our JSM (2.21).

To quantify the resolution capacity of our JSM (2.21), Fig. 4 displays the relative errors $e_{n,r}^\alpha$ $(n = 1, 2, \ldots, M)$ of (1.1) with $V(x) \equiv 0$ and different α under different DOFs M, i.e. $M = 512$, 2048 and 8192; and Fig. 5 shows similar results when $V(x) = \frac{x^2}{2}$.

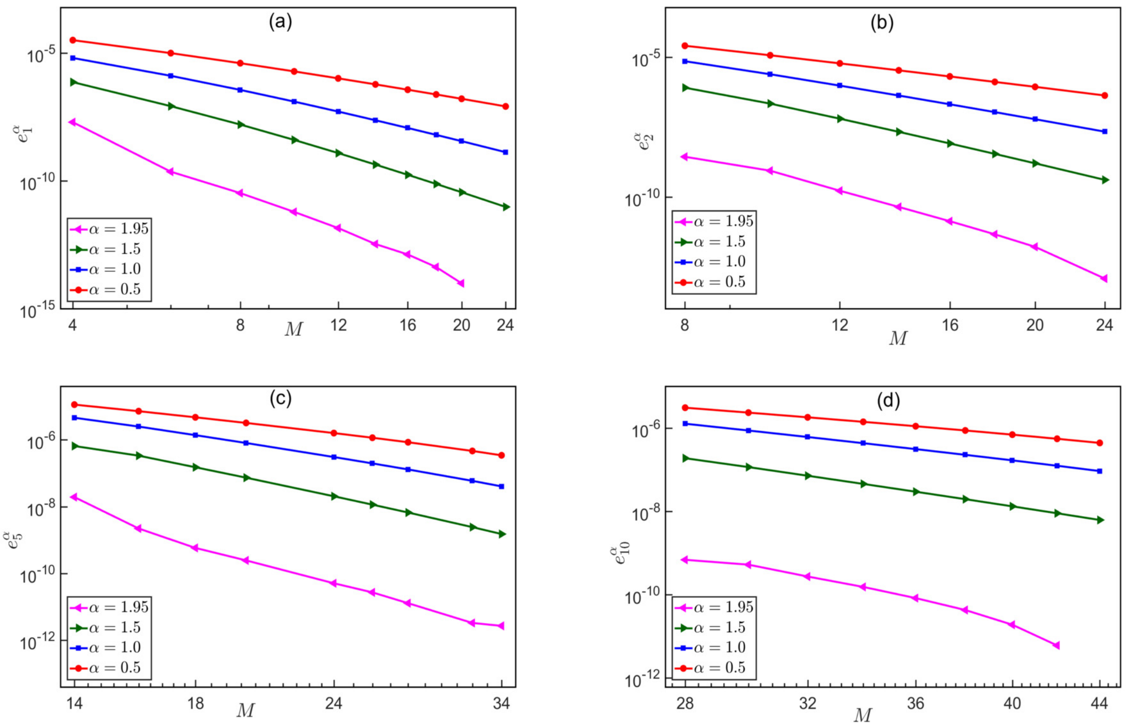

Fig. 1. Convergence rates of computing different eigenvalues of (1.1) with $\Omega = (-1, 1)$, $V(x) \equiv 0$ and different α by using our JSM (2.21) for: (a) the first eigenvalue λ_1^α, (b) the second eigenvalue λ_2^α, (c) the fifth eigenvalue λ_5^α, and (d) the tenth eigenvalue λ_{10}^α.

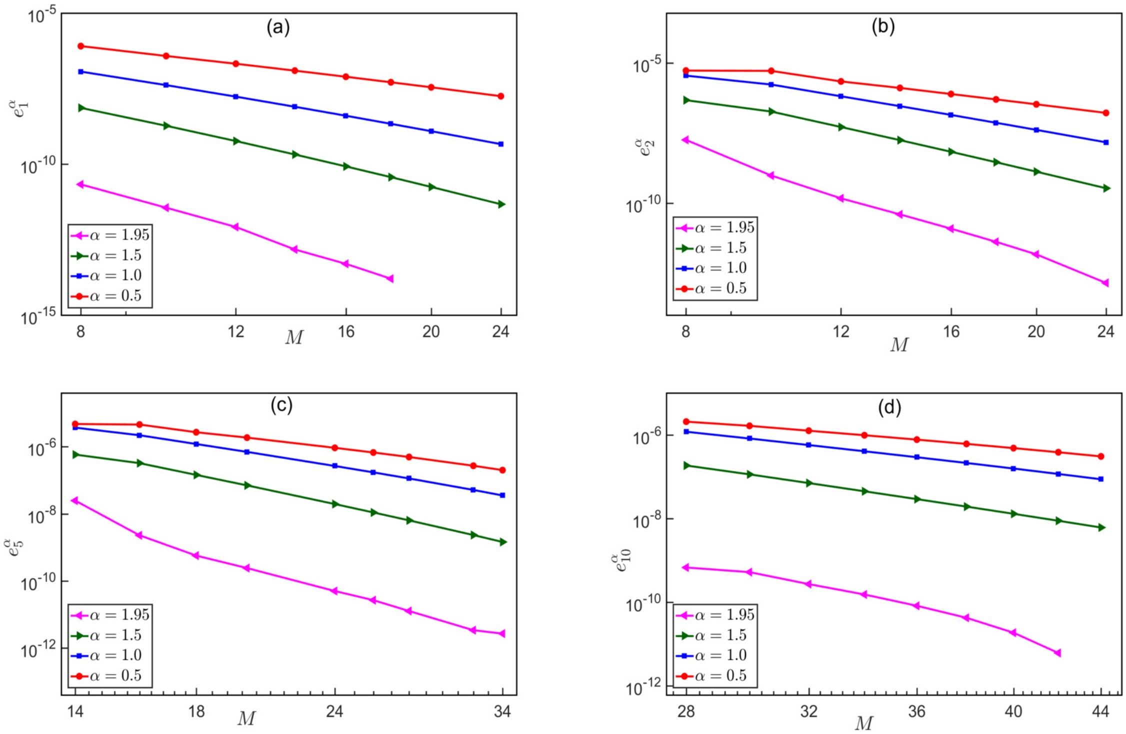

Fig. 2. Convergence rates of computing different eigenvalues of (1.1) with $\Omega = (-1, 1)$, $V(x) = \frac{x^2}{2}$ and different α by using our JSM (2.21) for: (a) the first eigenvalue λ_1^α, (b) the second eigenvalue λ_2^α, (c) the fifth eigenvalue λ_5^α, and (d) the tenth eigenvalue λ_{10}^α.

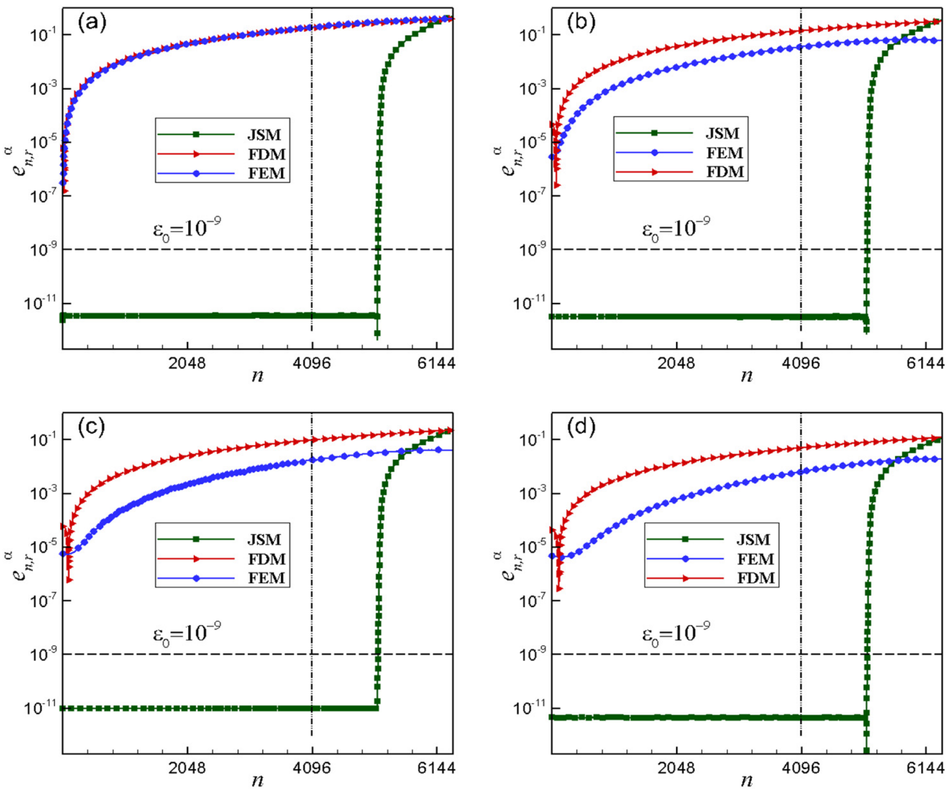

Fig. 3. Relative errors of the first 6400 eigenvalues, i.e. $e^{\alpha}_{n,r}$ ($n = 1, 2, \ldots, 6400$) of (1.1) with $\Omega = (-1, 1)$ and $V(x) \equiv 0$ by using our JSM (2.21), the FEM [41] and the FDM [69,22] under the DOF $M = 8192$ for: (a) $\alpha = 1.95$, (b) $\alpha = 1.5$, (c) $\alpha = 1.0$, and (d) $\alpha = 0.5$. A horizonal (dash) line with $\varepsilon_0 := 10^{-9}$ and a vertical (dash) line with $n := M/2$ are added in each sub-figure.

From Figs. 4 & 5, we can see that our JSM (2.21) under a given DOF M has the following resolution capacity (or trust region)

$$e^{\alpha}_{n,r} := \frac{\left|\lambda^{\alpha}_n - \lambda^{\alpha}_{n,M}\right|}{\lambda^{\alpha}_n} \le \varepsilon_0 := 10^{-9}, \qquad n = 1, 2, \ldots, c_r M, \qquad \text{with} \quad c_r \approx \frac{2}{\pi} > \frac{1}{2}. \tag{3.2}$$

Based on our numerical results, c_r is almost independent of $\alpha \in (0, 2]$. In fact, when $\alpha = 2$, $c_r \approx \frac{2}{\pi}$ was rigorously proved in [66]. From our numerical results, $c_r \approx 0.633 \approx \frac{2}{\pi}$ when $\alpha = 1.95$, 1.5, 1.0 and 0.5 (cf. Figs. 4 & 5). Rigorous mathematical justification of the independence of c_r on $\alpha \in (0, 2]$ is on-going.

4. Numerical results of the FSO in 1D without potential

In this section, we report numerical results on the eigenvalues of (1.1) with $\Omega = (-1, 1)$ and $V(x) \equiv 0$ by using our JSM (2.21) under the DOF $M = 8192$. All results are based on the first 4096 eigenvalues, i.e. we use half of the eigenvalues obtained numerically to present the results and to calculate distribution statistics.

4.1. Eigenvalues and their approximations

Fig. 6a plots the eigenvalues λ^{α}_n ($n = 1, 2, \ldots$) and their leading order approximations as $\lambda^{\alpha}_n \approx \tilde{\lambda}^{\alpha}_n := \left(\frac{n\pi}{2}\right)^{\alpha}$ ($n = 1, 2, \ldots$), while $\tilde{\lambda}^{\alpha}_n$ ($n = 1, 2, \ldots$) are the eigenvalues of the *local fractional Laplacian operator* on $\Omega = (-1, 1)$ with homogeneous Dirichlet boundary condition [11]. Fig. 6b displays the relative errors of the eigenvalues and their leading order approximations, i.e. $\tilde{e}^{\alpha}_{n,r} := \left(\tilde{\lambda}^{\alpha}_n - \lambda^{\alpha}_n\right)/\tilde{\lambda}^{\alpha}_n$, which immediately suggests a high order approximation at $\lambda^{\alpha}_n \approx \hat{\lambda}^{\alpha}_n := \tilde{\lambda}^{\alpha}_n \left(1 - \frac{C^{\alpha}_3}{n}\right)$ ($n = 1, 2, \ldots$). By fitting our numerical results, we can obtain numerically $C^{\alpha}_3 = \frac{\alpha(2-\alpha)}{4}$ which is plotted in Fig. 6c. Finally Fig. 6d displays the absolute errors of the eigenvalues and their high order approximations, i.e. $\tilde{e}^{\alpha}_n := \left|\lambda^{\alpha}_n - \hat{\lambda}^{\alpha}_n\right|$.

From Fig. 6, we can obtain numerically the following approximations of the eigenvalues of (1.1) with $\Omega = (-1, 1)$ and $V(x) \equiv 0$ as

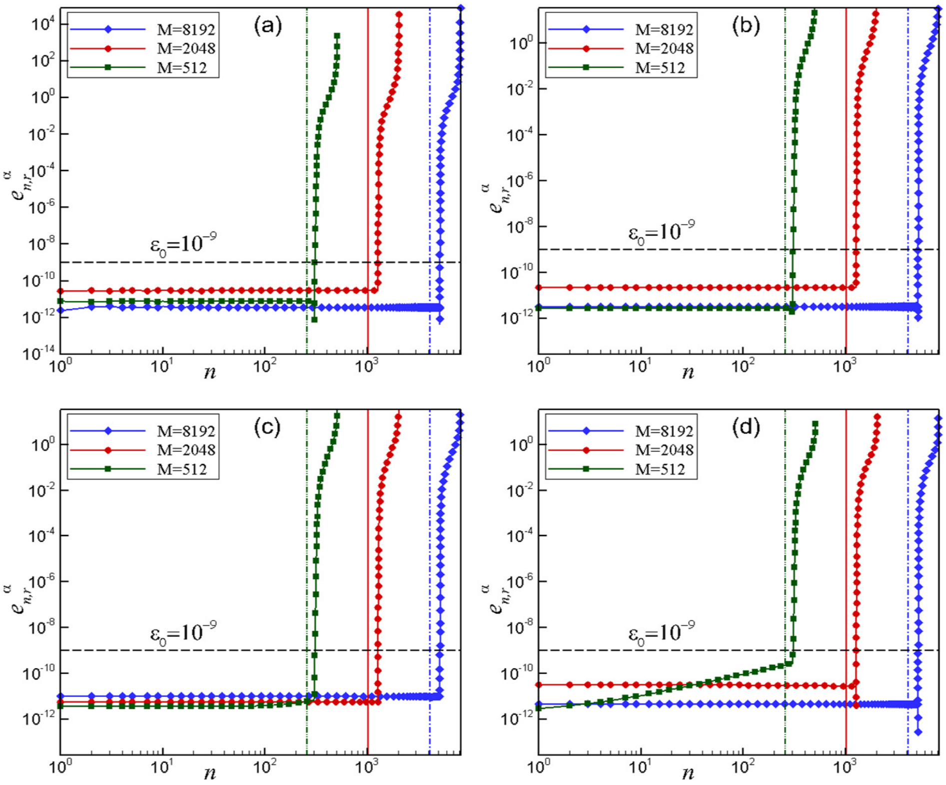

Fig. 4. Relative errors of the eigenvalues of (1.1) with $\Omega = (-1, 1)$ and $V(x) \equiv 0$ by using our JSM (2.21) under different DOFs M for: (a) $\alpha = 1.95$, (b) $\alpha = 1.5$, (c) $\alpha = 1.0$, and (d) $\alpha = 0.5$. A horizonal (dash) line with $\varepsilon_0 := 10^{-9}$ and vertical (dash) lines with $n := M/2$ are added in each sub-figure.

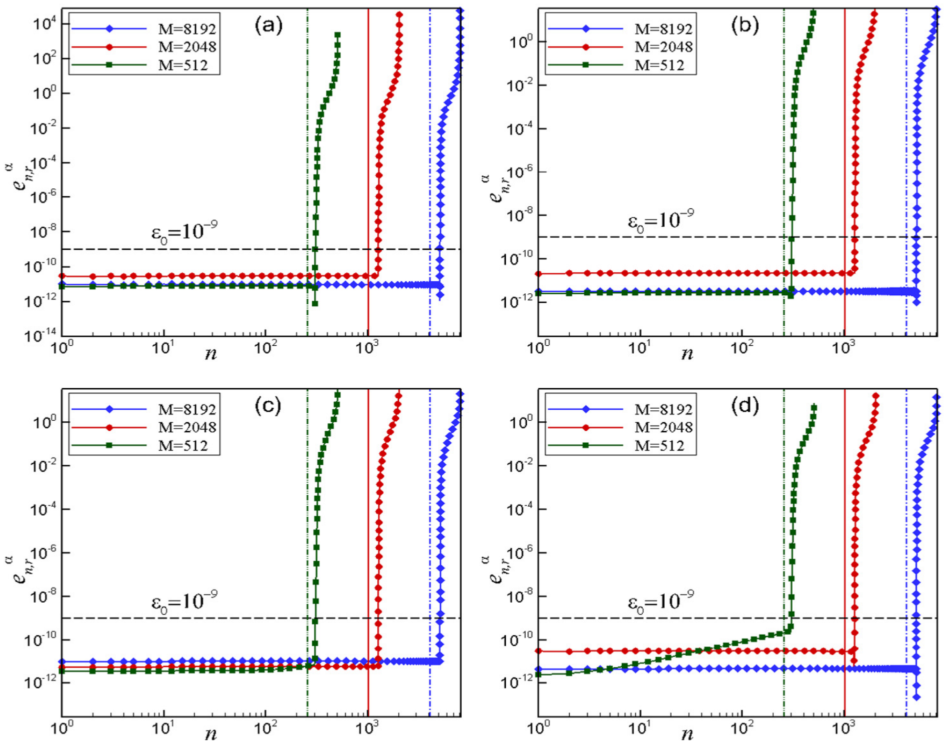

Fig. 5. Relative errors of the eigenvalues of (1.1) with $\Omega = (-1, 1)$ and $V(x) = \frac{x^2}{2}$ by using our JSM (2.21) under different DOFs M for: (a) $\alpha = 1.95$, (b) $\alpha = 1.5$, (c) $\alpha = 1.0$, and (d) $\alpha = 0.5$. A horizonal (dash) line with $\varepsilon_0 := 10^{-9}$ and vertical (dash) lines with $n := M/2$ are added in each sub-figure.

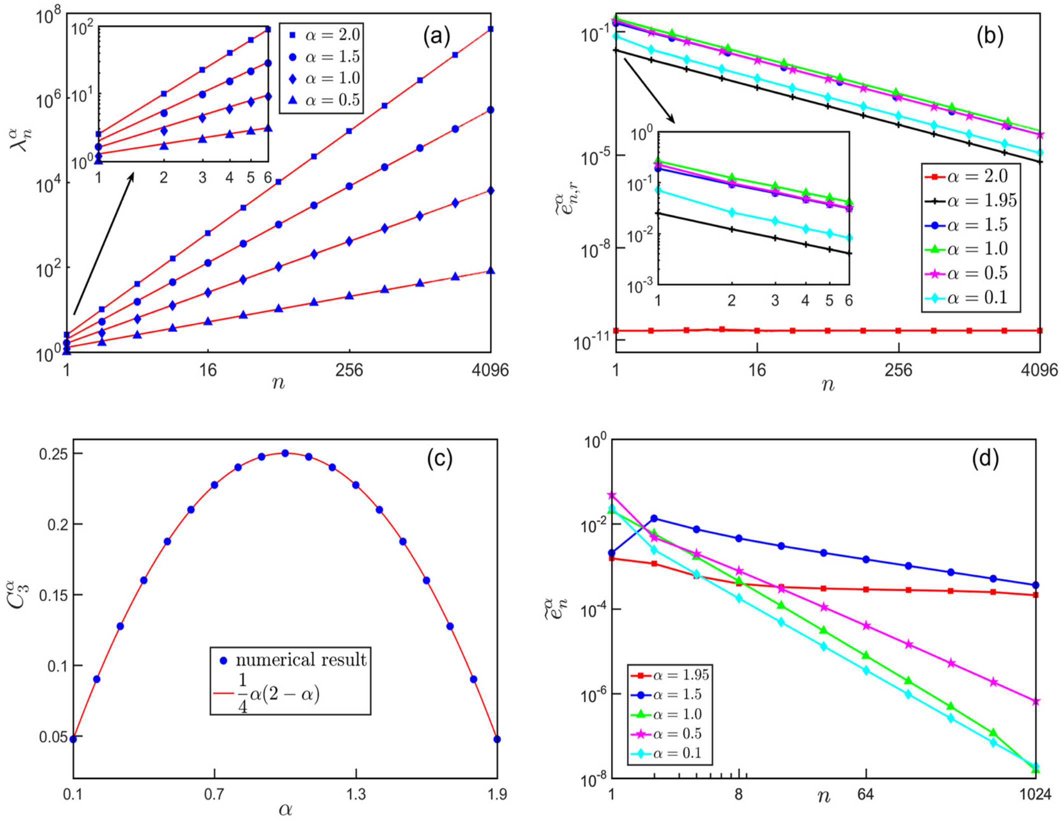

Fig. 6. (a) Eigenvalues λ_n^α $(n = 1, 2, \dots, 4096)$ of (1.1) with $\Omega = (-1, 1)$ and $V(x) \equiv 0$ for different α (symbols denote numerical results and solid lines are from the leading order approximation $\tilde{\lambda}_n^\alpha = \left(\frac{n\pi}{2}\right)^\alpha$); (b) Relative errors $\tilde{e}_{n,r}^\alpha = \left(\tilde{\lambda}_n^\alpha - \lambda_n^\alpha\right)/\tilde{\lambda}_n^\alpha$ (symbols denote numerical results and solid lines are from the fitting formula $C_3^\alpha n^{-1}$ when $n \gg 1$); (c) Fitting results for C_3^α; and (d) absolute errors $\tilde{e}_n^\alpha = \left|\lambda_n^\alpha - \hat{\lambda}_n^\alpha\right|$ with $\hat{\lambda}_n^\alpha = \tilde{\lambda}_n^\alpha\left(1 - C_3^\alpha n^{-1}\right)$.

$$\lambda_n^\alpha = \hat{\lambda}_n^\alpha + O(n^{\alpha-2}) = \tilde{\lambda}_n^\alpha\left[1 - \frac{\alpha(2-\alpha)}{4n} + O(n^{-2})\right], \quad n = 1, 2, \dots, \tag{4.1}$$

where

$$\tilde{\lambda}_n^\alpha = \left(\frac{n\pi}{2}\right)^\alpha, \quad \hat{\lambda}_n^\alpha = \left(\frac{n\pi}{2}\right)^\alpha - \left(\frac{\pi}{2}\right)^\alpha \frac{\alpha(2-\alpha)}{4} n^{\alpha-1} = \tilde{\lambda}_n^\alpha\left[1 - \frac{\alpha(2-\alpha)}{4n}\right], \quad n \geq 1, \quad 0 < \alpha \leq 2. \tag{4.2}$$

Combining (4.1) and Lemma 2.1, we can immediately obtain the conclusion (1.16).

To demonstrate high accuracy of our numerical method, Table 4 lists the eigenvalues of (1.1) with $\Omega = (-1, 1)$ and $V(x) \equiv 0$ for different α.

4.2. Asymptotic behaviour of different gaps

Fig. 7 plots different eigenvalue gaps of (1.1) with $\Omega = (-1, 1)$, $V(x) \equiv 0$ and different α. From Fig. 7, we can draw the following conclusions based on our numerical results: (i) the nearest neighbour gaps $\delta_{\rm nn}^\alpha(N)$ increase and decrease with respect to N when $1 < \alpha \leq 2$ and $0 < \alpha < 1$, respectively; and they are almost constant when $\alpha = 1$ (cf. Fig. 7a). (ii) The minimum gaps $\delta_{\rm min}^\alpha(N)$ are almost constants and decrease with respect to N when $1 \leq \alpha \leq 2$ and $0 < \alpha < 1$, respectively (cf. Fig. 7b). (iii) The average gaps $\delta_{\rm ave}^\alpha(N)$ increase and decrease with respect to N when $1 < \alpha \leq 2$ and $0 < \alpha < 1$, respectively; and they are almost constant when $\alpha = 1$ (cf. Fig. 7c). (iv) The normalized gaps $\delta_{\rm norm}^\alpha(N) \approx 1$ when $N \gg 1$ (cf. Fig. 7d).

In fact, based on the numerical asymptotic approximation (4.1), we can formally obtain the following approximation of the nearest neighbour gaps as

$$\begin{aligned}\delta_{\rm nn}^\alpha(N) &= \lambda_{N+1}^\alpha - \lambda_N^\alpha \approx \hat{\lambda}_{N+1}^\alpha - \hat{\lambda}_N^\alpha \\ &= \left(\frac{(N+1)\pi}{2}\right)^\alpha - \left(\frac{\pi}{2}\right)^\alpha \frac{\alpha(2-\alpha)}{4}(N+1)^{\alpha-1} - \left(\frac{N\pi}{2}\right)^\alpha + \left(\frac{\pi}{2}\right)^\alpha \frac{\alpha(2-\alpha)}{4} N^{\alpha-1}\end{aligned}$$

Table 4
Eigenvalues of (1.1) with $\Omega = (-1, 1)$ and $V(x) \equiv 0$ for different α.

	$\alpha = 0.1$	$\alpha = 0.5$	$\alpha = 1.0$	$\alpha = 1.5$	$\alpha = 1.95$	$\alpha = 2.0$
λ_1^α	0.9725944	0.9701654	1.157773883	1.5975035456	2.35198053244	2.4674011002
λ_2^α	1.0921964	1.6015377	2.754754742	5.0597599283	9.20812426623	9.8696044010
λ_3^α	1.1473224	2.0288210	4.316801066	9.5943057675	20.3833201062	22.206609902
λ_4^α	1.1868395	2.3871563	5.892147470	15.018786212	35.7934316323	39.478417604
λ_5^α	1.2165513	2.6947426	7.460175739	21.189425897	55.3737634238	61.685027506
λ_6^α	1.2412799	2.9728959	9.032852690	28.035207791	79.0793754673	88.826439609
λ_7^α	1.2619743	3.2256090	10.60229309	35.488011031	106.871259423	120.90265391
λ_8^α	1.2801923	3.4610502	12.17411826	43.507108689	138.718756729	157.91367041
λ_9^α	1.2961956	3.6805940	13.74410905	52.051027490	174.594065184	199.85948912
λ_{10}^α	1.3107082	3.8884472	15.31555499	61.092457389	214.473975149	246.74011002
λ_{20}^α	1.4082270	5.5522311	31.02330309	174.43784577	829.684155066	986.96044010
λ_{40}^α	1.5111219	7.8894197	62.43917339	495.95713648	3207.64320222	3947.8417604
λ_{60}^α	1.5742803	9.6777480	93.85508924	912.11187382	7073.79138904	8882.6439609

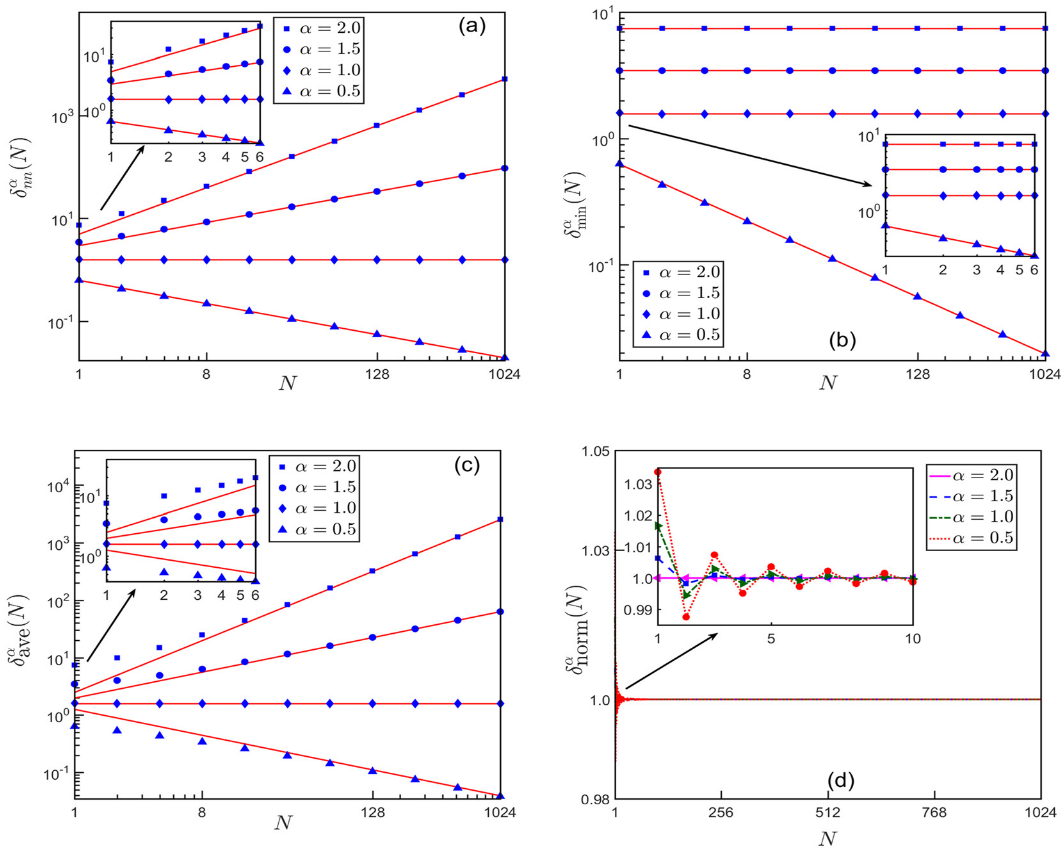

Fig. 7. Different eigenvalue gaps of (1.1) with $\Omega = (-1, 1)$, $V(x) \equiv 0$ and different α for (symbols denote numerical results and solid lines are from fitting formulas when $N \gg 1$): (a) the nearest neighbour gaps $\delta_{\mathrm{nn}}^\alpha(N)$, (b) the minimum gaps $\delta_{\min}^\alpha(N)$, (c) the average gaps $\delta_{\mathrm{ave}}^\alpha(N)$, and (d) the normalized gaps $\delta_{\mathrm{norm}}^\alpha(N)$.

$$
\begin{aligned}
&= \left(\frac{\pi}{2}\right)^\alpha \left[(N+1)^\alpha - N^\alpha - \frac{\alpha(2-\alpha)}{4}\left((N+1)^{\alpha-1} - N^{\alpha-1}\right)\right] \\
&= \left(\frac{\pi}{2}\right)^\alpha \left[N^\alpha\left(\left(1+\frac{1}{N}\right)^\alpha - 1\right) - \frac{\alpha(2-\alpha)}{4}N^{\alpha-1}\left(\left(1+\frac{1}{N}\right)^{\alpha-1} - 1\right)\right] \\
&= \left(\frac{\pi}{2}\right)^\alpha \left[N^\alpha\left(\frac{\alpha}{N} + \frac{\alpha(\alpha-1)}{N^2} + O(N^{-3})\right) - \frac{\alpha(2-\alpha)}{4}N^{\alpha-1}\left(\frac{\alpha-1}{N} + O(N^{-2})\right)\right]
\end{aligned}
$$

$$= \left(\frac{\pi}{2}\right)^{\alpha}\left[\alpha N^{\alpha-1} + \frac{\alpha(\alpha-1)(2+\alpha)}{4}N^{\alpha-2} + O(N^{\alpha-3})\right], \qquad N = 1, 2, \dots . \tag{4.3}$$

Again, this asymptotic results also confirm that the nearest neighbour gaps $\delta_{\rm nn}^{\alpha}(N)$ increase and decrease with respect to N when $1 < \alpha \le 2$ and $0 < \alpha < 1$, respectively; and they are almost constant when $\alpha = 1$.

Based on the asymptotic results (4.3) and the numerical results in Fig. 7b, we can conclude that

$$\delta_{\min}^{\alpha}(N) = \begin{cases} \delta_{\rm nn}^{\alpha}(1) = \lambda_2^{\alpha} - \lambda_1^{\alpha}, & 1 < \alpha < 2, \\ \approx \delta_{\rm nn}^{\alpha}(1) = \lambda_2^{\alpha} - \lambda_1^{\alpha}, & \alpha = 1, \\ \delta_{\rm nn}^{\alpha}(N) \approx \alpha\left(\frac{\pi}{2}\right)^{\alpha} N^{\alpha-1}, & 0 < \alpha < 1. \end{cases} \qquad N = 1, 2, \dots . \tag{4.4}$$

Again, these asymptotic results suggest that the minimum gaps $\delta_{\min}^{\alpha}(N)$ are almost constants and decrease with respect to N when $1 \le \alpha \le 2$ and $0 < \alpha < 1$, respectively.

Similarly, we have the asymptotic results for the average gaps as

$$\begin{aligned} \delta_{\rm ave}^{\alpha}(N) &= \frac{\lambda_{N+1}^{\alpha} - \lambda_1^{\alpha}}{N} \approx \frac{\hat{\lambda}_{N+1}^{\alpha} - \lambda_1^{\alpha}}{N} \\ &= \frac{1}{N}\left[\left(\frac{(N+1)\pi}{2}\right)^{\alpha} - \left(\frac{\pi}{2}\right)^{\alpha}\frac{\alpha(2-\alpha)}{4}(N+1)^{\alpha-1} - \lambda_1^{\alpha}\right] \\ &= \left(\frac{\pi}{2}\right)^{\alpha}\left[N^{\alpha-1}\left(1+\frac{1}{N}\right)^{\alpha} - \frac{\alpha(2-\alpha)}{4}N^{\alpha-2}\left(1+\frac{1}{N}\right)^{\alpha-1} - \lambda_1^{\alpha}\left(\frac{2}{\pi}\right)^{\alpha}N^{-1}\right] \\ &= \left(\frac{\pi}{2}\right)^{\alpha}\left[N^{\alpha-1} + \alpha N^{\alpha-2} - \frac{\alpha(2-\alpha)}{4}N^{\alpha-2} - \lambda_1^{\alpha}\left(\frac{2}{\pi}\right)^{\alpha}N^{-1} + O(N^{\alpha-3})\right] \\ &= \left(\frac{\pi}{2}\right)^{\alpha}\left[N^{\alpha-1} + \frac{\alpha(2+\alpha)}{4}N^{\alpha-2} - \lambda_1^{\alpha}\left(\frac{2}{\pi}\right)^{\alpha}N^{-1} + O(N^{\alpha-3})\right], \qquad N = 1, 2, \dots . \end{aligned} \tag{4.5}$$

Thus when $1 < \alpha < 2$, we have

$$\delta_{\rm ave}^{\alpha}(N) = \left(\frac{\pi}{2}\right)^{\alpha}\left[N^{\alpha-1} + \frac{\alpha(2+\alpha)}{4}N^{\alpha-2} + O(N^{-1})\right], \qquad N = 1, 2, \dots ; \tag{4.6}$$

and when $0 < \alpha < 1$, we have

$$\delta_{\rm ave}^{\alpha}(N) = \left(\frac{\pi}{2}\right)^{\alpha}\left[N^{\alpha-1} - \lambda_1^{\alpha}\left(\frac{2}{\pi}\right)^{\alpha}N^{-1} + O(N^{\alpha-2})\right], \qquad N = 1, 2, \dots ; \tag{4.7}$$

and when $\alpha = 1$, we get

$$\delta_{\rm ave}^{\alpha}(N) = \frac{\pi}{2}\left[1 + \left(\frac{3}{4} - \frac{2}{\pi}\lambda_1^{\alpha=1}\right)N^{-1} + O(N^{-2})\right], \qquad N = 1, 2, \dots . \tag{4.8}$$

Again, these asymptotic results suggest that the average gaps $\delta_{\rm ave}^{\alpha}(N)$ increase and decrease with respect to N when $1 < \alpha \le 2$ and $0 < \alpha < 1$, respectively; and they are almost constants when $\alpha = 1$ (cf. Fig. 7c).

Based on the asymptotic results of the eigenvalue λ_n^{α} in (4.1), noticing (1.8)-(1.10), we can get the asymptotic results for the normalized gaps as

$$\begin{aligned} \delta_{\rm norm}^{\alpha}(N) &= \frac{2}{\pi}\left[\left(\lambda_{N+1}^{\alpha}\right)^{1/\alpha} - \left(\lambda_N^{\alpha}\right)^{1/\alpha}\right] \\ &= (N+1)\left(1 - \frac{\alpha(2-\alpha)}{4(N+1)} + O((N+1)^{-2})\right)^{1/\alpha} - N\left(1 - \frac{\alpha(2-\alpha)}{4N} + O(N^{-2})\right)^{1/\alpha} \\ &= N + 1 - \frac{2-\alpha}{4} - \frac{\tilde{C}}{N+1} + O((N+1)^{-2}) - N + \frac{2-\alpha}{4} + \frac{\tilde{C}}{N} - O(N^{-2}) \\ &= 1 + \frac{\tilde{C}}{N(N+1)} + O(N^{-3}), \qquad N = 1, 2, \dots , \end{aligned} \tag{4.9}$$

where $\tilde{C}$ is a constant. Again, this asymptotic result suggests that the normalized gaps $\delta_{\rm norm}^{\alpha}(N) \approx 1$ when $N \gg 1$ (cf. Fig. 7d).

Finally, combining (4.3), (4.4), (4.6), (4.7), (4.8), (4.9) and (2.3), we can get the conjecture (1.17) stated in Section 1.

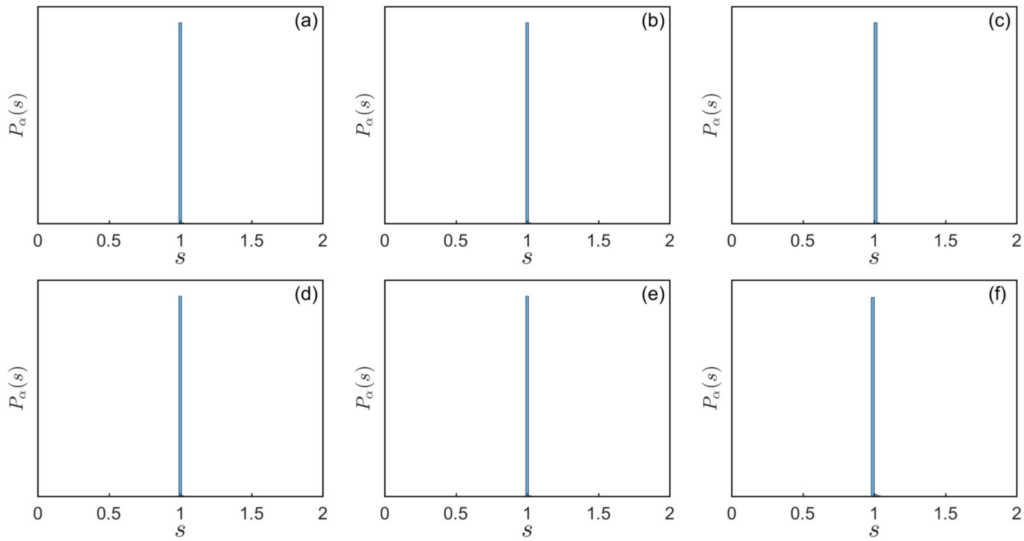

Fig. 8. The histogram of the normalized gaps $\{\delta^\alpha_{\rm norm}(n) \mid 1 \le n \le N = 4096\}$ of (1.1) with $\Omega = (-1, 1)$ and $V(x) \equiv 0$ for different α: (a) $\alpha = 2.0$, (b) $\alpha = 1.9$, (c) $\alpha = \sqrt{3}$, (d) $\alpha = 1.5$, (e) $\alpha = 1.0$, and (f) $\alpha = 0.5$.

4.3. The gaps distribution statistics

Fig. 8 displays the histogram of the normalized gaps $\{\delta^\alpha_{\rm norm}(n) \mid 1 \le n \le N = 4096\}$ defined in (4.9) for (1.1) with $\Omega = (-1, 1)$, $V(x) \equiv 0$ and different α.

From Fig. 8, we can conclude that the gaps distribution statistics of (1.1) with $V(x) \equiv 0$ is $P_\alpha(s) = \delta(s-1)$ for $0 < \alpha \le 2$.

4.4. Eigenfunctions and their singularity characteristics

Denote $u^\alpha_n(x)$ be the eigenfunction satisfying $\|u^\alpha_n\|_{L^2(\Omega)} = 1$ and $\left.\frac{du^\alpha_n(x)}{dx}\right|_{x=-1} > 0$, which corresponds to the eigenvalue λ^α_n $(n = 1, 2, \dots)$ of (1.1) with $\Omega = (-1, 1)$ and $V(x) \equiv 0$. The 'exact' eigenfunctions $u^\alpha_n(x)$ $(n = 1, 2, \dots)$ are obtained numerically by using the JSM (2.21) under a very large DOF $M = M_0$, e.g. $M_0 = 512$. Let $u^\alpha_{n,M}(x)$ be the numerical approximation of $u^\alpha_n(x)$ $(n = 1, 2, \dots, M)$ obtained by a numerical method with the DOF chosen as M. Define the absolute errors of $u^\alpha_n(x)$ as

$$e_{u^\alpha_n} := \|u^\alpha_n - u^\alpha_{n,M}\|_{l^2}, \qquad n = 1, 2, \dots . \tag{4.10}$$

Fig. 9 shows convergence rates of our JSM (2.21) for computing the first, second, fifth and tenth eigenfunctions of (1.1) with $\Omega = (-1, 1)$, $V(x) \equiv 0$ and different α. Fig. 10 plots different eigenfunctions of (1.1) with $\Omega = (-1, 1)$, $V(x) \equiv 0$ and different α. Finally Fig. 11 displays different eigenfunctions of (1.1) with $\Omega = (-1, 1)$, $V(x) \equiv 0$ and different α near the boundary layer $0 < \xi := x + 1 \ll 1$ to show the singularity characteristics of the eigenfunctions $u^\alpha_n(x)$ at the boundary $x = -1$.

From Figs. 9–11, we can draw the following conclusions: (i) Our JSM method (2.21) converges sub-spectrally (or super-linearly) with respect to the DOF M for computing the eigenfunctions $u^\alpha_n(x)$ (cf. Fig. 9). (ii) For fixed $0 < \alpha < 2$, the eigenfunctions $u^\alpha_n(x)$ $(n = 1, 2, \dots)$ can be characterised as

$$u^\alpha_n(x) = (1 - x^2)^{\alpha/2}\, v^\alpha_n(x), \qquad -1 \le x \le 1, \tag{4.11}$$

where $v^\alpha_n(x)$ $(n = 1, 2, \dots)$ are smooth functions over the interval $\bar{\Omega} = [-1, 1]$ (cf. Fig. 11). In addition, our numerical results indicate that, when $n \to \infty$ (cf. Fig. 10d), the eigenfunctions $u^\alpha_n(x)$ $(n \ge 1)$ of (1.1) with $\Omega = (-1, 1)$ and $V(x) \equiv 0$ converge to the eigenfunctions $u^{\alpha=2}_n(x) = \sin\left(\frac{n\pi(x+1)}{2}\right)$ $(n \ge 1)$ of (1.1) with $\alpha = 2$, $\Omega = (-1, 1)$ and $V(x) \equiv 0$, i.e.

$$u^\alpha_n(x) \to \sin\left(\frac{n\pi(x+1)}{2}\right) = u^{\alpha=2}_n(x), \qquad x \in \bar{\Omega}, \qquad n \to \infty. \tag{4.12}$$

Based on the above results, for the eigenvalue problem of the FSO in high dimensions, i.e.

Find $\lambda \in \mathbb{R}$ and a nonzero real-valued function $u(\mathbf{x}) \neq 0$ such that

$$\begin{aligned} &L_{\rm FSO}\, u(\mathbf{x}) := \left[(-\Delta)^{\alpha/2} + V(\mathbf{x})\right] u(\mathbf{x}) = \lambda\, u(\mathbf{x}), \qquad \mathbf{x} \in \Omega \subset \mathbb{R}^d, \\ &\quad u(\mathbf{x}) = 0, \qquad \mathbf{x} \in \Omega^c := \mathbb{R}^d \backslash \Omega, \end{aligned} \tag{4.13}$$

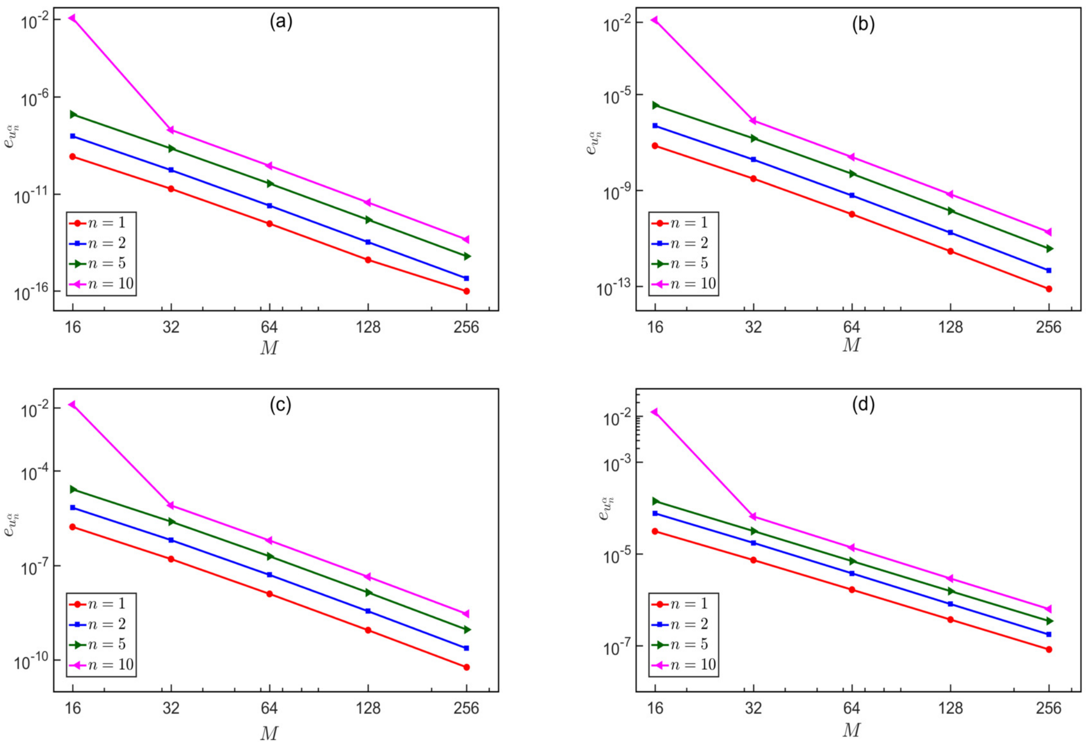

Fig. 9. Convergence rates of computing different eigenfunctions $u_n^\alpha(x)$ ($n = 1, 2, 5, 10$) of (1.1) with $\Omega = (-1, 1)$ and $V(x) \equiv 0$ by using our JSM (2.21) for different α: (a) $\alpha = 1.95$, (b) $\alpha = 1.5$, (c) $\alpha = 1.0$ and (d) $\alpha = 0.5$.

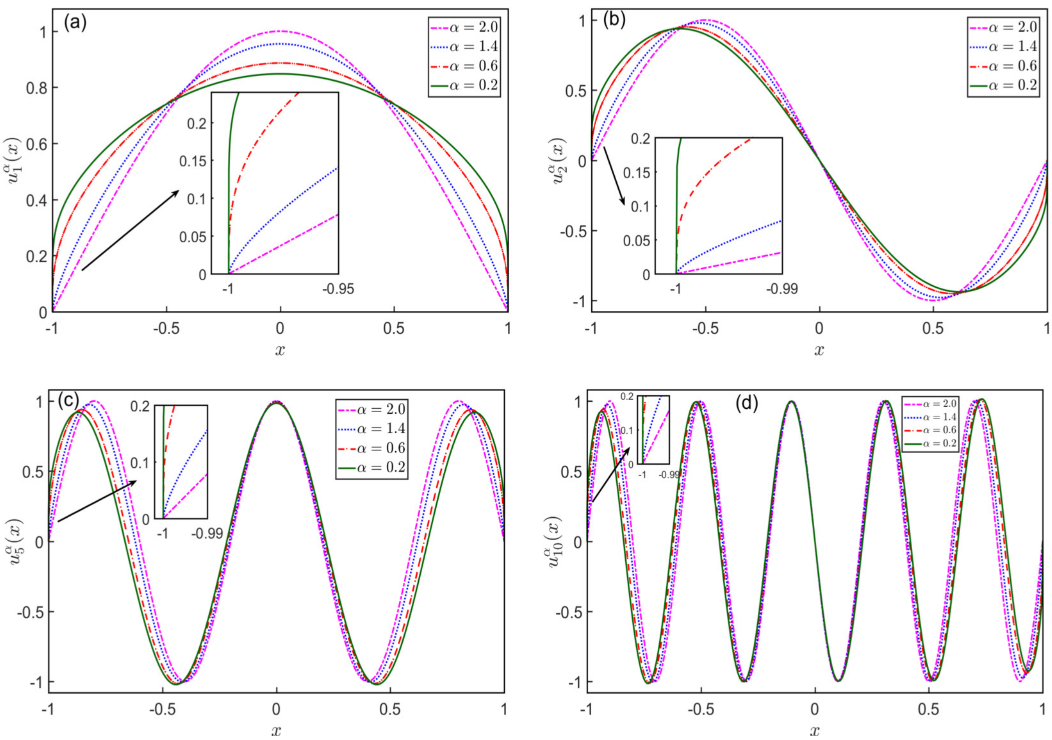

Fig. 10. Plots of different eigenfunctions of (1.1) with $\Omega = (-1, 1)$, $V(x) \equiv 0$ and different α for: (a) the first eigenfunction $u_1^\alpha(x)$, (b) the second eigenfunction $u_2^\alpha(x)$, (c) the fifth eigenfunction $u_5^\alpha(x)$, and (d) the tenth eigenfunction $u_{10}^\alpha(x)$.

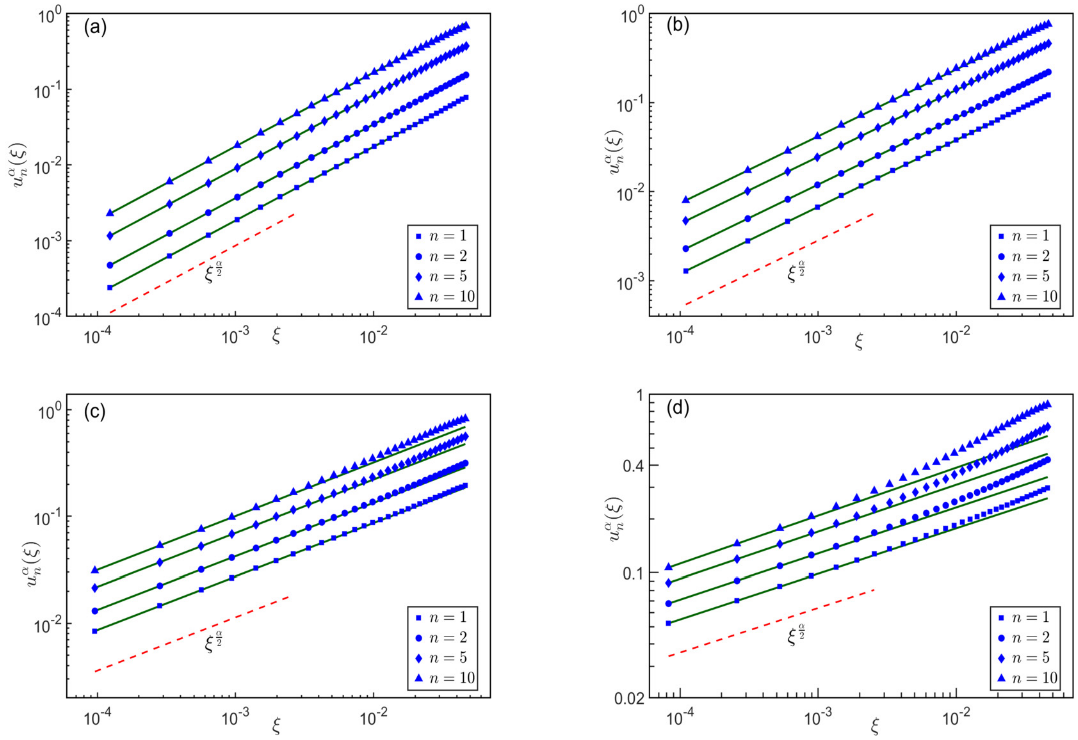

Fig. 11. Singularity characteristics of different eigenfunctions of (1.1) with $\Omega = (-1, 1)$ and $V(x) \equiv 0$ (symbols denote numerical results and solid lines are from the fitting formula $C\xi^{\alpha/2}$ when $0 < \xi = x + 1 \ll 1$) for different α: (a) $\alpha = 1.95$, (b) $\alpha = 1.5$, (c) $\alpha = 1.0$ and (d) $\alpha = 0.5$.

where $d \ge 2$, $0 < \alpha < 2$, Ω is a bounded domain and the fractional Laplacian $(-\Delta)^{\alpha/2}$ is defined via the Fourier transform [19,54], we conjecture here that the eigenfunction $u(\mathbf{x})$ can be written as

$$u(\mathbf{x}) = v(\mathbf{x})\,(\mathrm{dist}(\mathbf{x}, \partial\Omega))^{\alpha/2}, \qquad \mathbf{x} \in \bar{\Omega}, \tag{4.14}$$

where $v(\mathbf{x})$ is a smooth function over $\bar{\Omega}$ and $\mathrm{dist}(\mathbf{x}, \partial\Omega)$ represents the distance from $\mathbf{x} \in \Omega$ to $\partial\Omega$.

We remark here that the singularity characteristics of the eigenfunctions in (4.11) for 1D (or (4.14) for high dimensions) is quite different with the singularity characteristics given in [16] for fractional PDEs as

$$u(\mathbf{x}) \approx (\mathrm{dist}(\mathbf{x}, \partial\Omega))^{\alpha/2} + v(\mathbf{x}), \qquad \mathbf{x} \in \bar{\Omega}, \tag{4.15}$$

where $v(\mathbf{x})$ is a smooth function over $\bar{\Omega}$. From our numerical results, we speculate that the correct singularity characteristics of the solutions of the fractional PDEs should be (4.14) instead of (4.15)!

5. Numerical results of the FSO in 1D with potential

In this section, we report numerical results on the eigenvalues of (1.1) with $\Omega = (-1, 1)$ and $V(x) \neq 0$ by using our JSM (2.21) under the DOF $M = 8192$. All results are based on the first 4096 eigenvalues, i.e. we use half of the eigenvalues obtained numerically to present the results and to calculate gaps distribution statistics. Here we consider four different external potentials given as:

Case I. $V(x) = \frac{x^2}{2}$;
Case II. $V(x) = 4x^2$;
Case III. $V(x) = 4x^2 + \sin(\frac{\pi}{2}x)$;
Case IV. $V(x) = 50x^2 + \sin(2\pi x)$.

5.1. Eigenvalues and their asymptotics

Table 5 lists the eigenvalues of (1.1) with $\Omega = (-1, 1)$ and $V(x) = \frac{x^2}{2}$ for different α. Fig. 12 plots the eigenvalues of (1.1) with $\Omega = (-1, 1)$, different external potentials $V(x)$ and different α.

From Fig. 12, we can conclude that, when $n \gg 1$, the leading order asymptotics of the eigenvalues λ_n^α in (4.1) is still valid for the eigenvalue problem of the FSO (1.1) with potential $V(x)$.

Table 5
Different eigenvalues of (1.1) with $\Omega = (-1, 1)$, $V(x) = \frac{x^2}{2}$ and different α obtained numerically by our JSM (2.21).

	$\alpha = 0.5$	$\alpha = 1.0$	$\alpha = 1.5$	$\alpha = 1.9$	$\alpha = 2.0$
λ_1^α	1.0599238	1.240244372	1.6707307180	2.31063679348	2.53245197432
λ_2^α	1.7684725	2.918074603	5.2120578091	8.73899699079	10.0106621605
λ_3^α	2.1903345	4.481368142	9.7550085449	18.8734566366	22.3620761310
λ_4^α	2.5518267	6.058660406	15.182580104	32.6230979973	39.6388288214
λ_5^α	2.8580498	7.626501974	21.354271585	49.8832020720	61.8477048695
λ_6^α	3.1370031	9.199495156	28.200700106	70.5802261928	88.9903414346
λ_7^α	3.3893161	10.76885112	35.653816621	94.6494682651	121.067291745
λ_8^α	3.6251388	12.34077821	43.673146060	122.040857583	158.078785000
λ_9^α	3.8445549	13.91072820	52.217197374	152.708819987	200.024930128
λ_{10}^α	4.0526430	15.48221913	61.258734930	186.615849002	246.905784303
λ_{20}^α	5.5522311	31.02330310	174.43784577	697.513597025	986.960440109
λ_{40}^α	7.8894197	62.43917340	495.71364899	2606.30876720	3947.84176043
λ_{60}^α	9.6777480	93.85508927	912.11187382	5633.40862247	8882.64396098

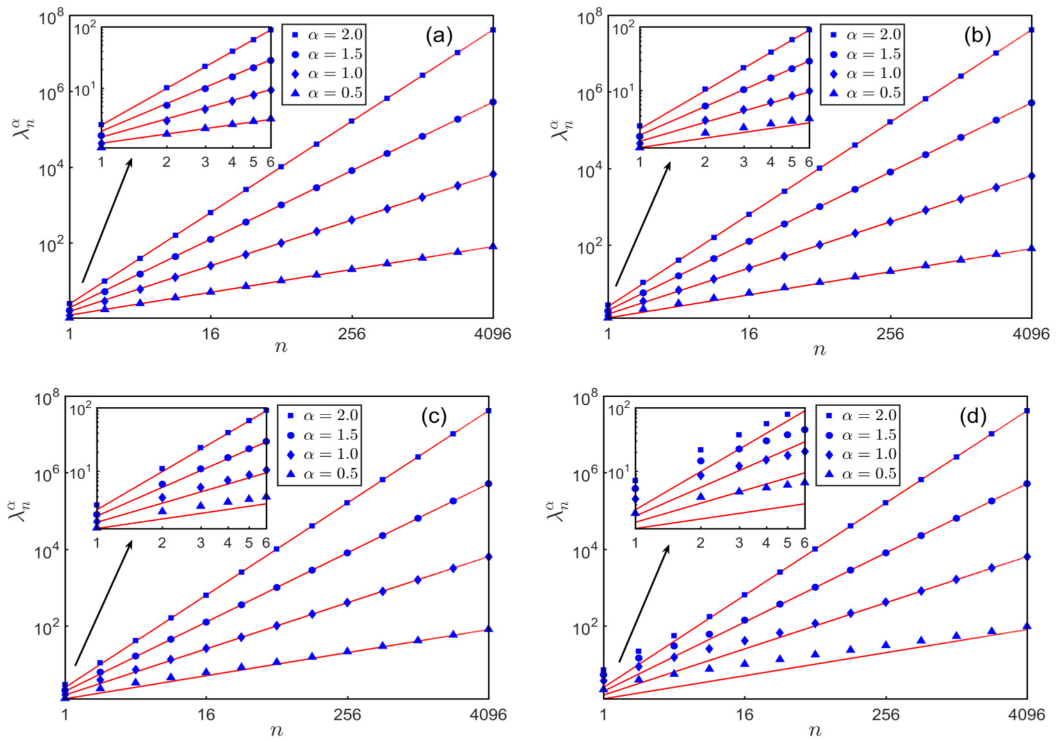

Fig. 12. Eigenvalues λ_n^α ($n = 1, 2, \dots, 4096$) of (1.1) with $\Omega = (-1, 1)$ and different α for differential external potentials (symbols denote numerical results and solid lines are from fitting formulas when $n \gg 1$): (a) Case I, (b) Case II, (c) Case III, and (d) Case IV.

5.2. Gaps and their distribution statistics

Fig. 13 plots different eigenvalue gaps of (1.1) with $\Omega = (-1, 1)$, $V(x) = \frac{x^2}{2}$ and different α. Fig. 14 displays the histogram of the normalized gaps $\{\delta_{\text{norm}}^\alpha(n) \mid 1 \le n \le N = 4096\}$ defined in (4.9) for (1.1) with $\Omega = (-1, 1)$, $V(x) = \frac{x^2}{2}$ and different α. For other potentials, our numerical results show similar behaviour on eigenvalues and their gaps, which are omitted here for brevity.

Again, from Figs. 13 and 14, we can conclude that, when $n \gg 1$, the asymptotics of the eigenvalue gaps given in (4.3), (4.4), (4.6), (4.7), (4.8) and (4.9) are still valid for the eigenvalue problem of the FSO (1.1) with potential $V(x)$. In addition, the gaps distribution statistics is still $P_\alpha(s) = \delta(s - 1)$ for $0 < \alpha \le 2$ in this case.

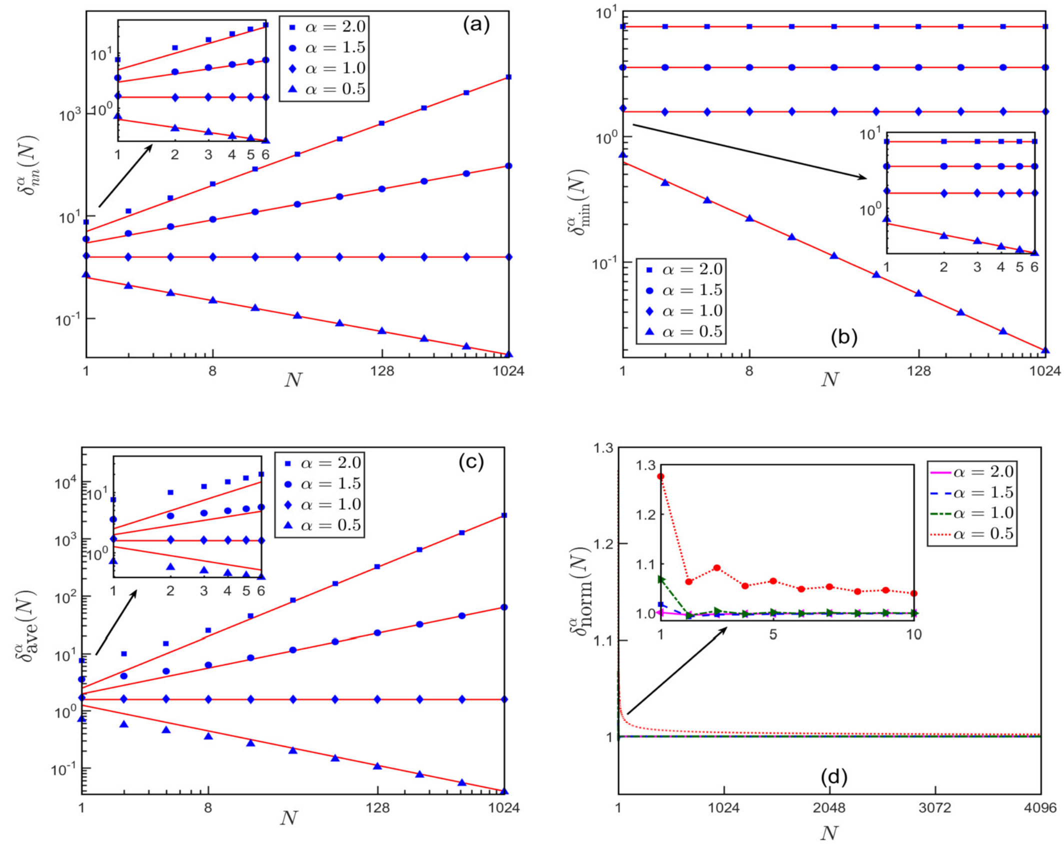

Fig. 13. Different eigenvalue gaps of (1.1) with $\Omega = (-1, 1)$, $V(x) = \frac{x^2}{2}$ and different α for (symbols denote numerical results and solid lines are from fitting formulas when $N \gg 1$ in a-c): (a) the nearest neighbour gaps $\delta_{\text{nn}}^{\alpha}(N)$, (b) the minimum gaps $\delta_{\min}^{\alpha}(N)$, (c) the average gaps $\delta_{\text{ave}}^{\alpha}(N)$, and (d) the normalized gaps $\delta_{\text{norm}}^{\alpha}(N)$.

5.3. *Comparison on eigenvalues of (1.1) without/with potential*

Let $0 < \lambda_1^{\alpha,0} < \lambda_2^{\alpha,0} < \ldots < \lambda_n^{\alpha,0} < \ldots$ be all eigenvalues of (1.1) with $\Omega = (-1, 1)$ and $V(x) \equiv 0$, and denote all eigenvalues of (1.1) with a potential V as in (1.4). Fig. 15 plots differences of the eigenvalues of (1.1) with the potential $V(x)$ and without potential, i.e. $\delta_n^V := \lambda_n^{\alpha} - \lambda_n^{\alpha,0} - C_V$ $(1 \le n \le N = 4096)$ for different potentials $V(x)$ and α, where $C_V = \frac{1}{2}\int_{-1}^{1} V(x)dx$.

From Fig. 15, we can draw the following conclusion for the eigenvalues of (1.1) with potential $V(x)$:

$$\lambda_n^{\alpha} = \lambda_n^{\alpha,0} + C_V + O\left(n^{-\tau_1(\alpha)}\right), \qquad n \gg 1, \tag{5.1}$$

where $\tau_1(\alpha)$ can be obtained numerically as

$$\tau_1(\alpha) = \begin{cases} \alpha, & 0 < \alpha \le 2 \& \alpha \ne 1, \\ \approx 4.5, & \alpha = 1, \end{cases} \tag{5.2}$$

5.4. *Eigenfunctions*

Fig. 16 plots different eigenfunctions $u_n^{\alpha}(x)$ of (1.1) with $\Omega = (-1, 1)$ and $V(x) = \frac{x^2}{2}$ for different α.

From Fig. 16, the singularity characteristics of the eigenfunctions given in (4.11) is still valid for the eigenvalue problem of the FSO (1.1) with potential $V(x)$. In addition, when $0 < \alpha < 2$, our numerical results indicate that, when $n \to \infty$ (cf. Fig. 10d), the eigenfunctions $u_n^{\alpha}(x)$ $(n \ge 1)$ of (1.1) with potential $V(x)$ converge to the eigenfunctions $u_n^{\alpha=2}(x) = \sin\left(\frac{n\pi(x+1)}{2}\right)$ $(n \ge 1)$ which are the eigenfunctions of (1.1) with $\alpha = 2$ and $V(x) \equiv 0$.

Finally, based on our extensive numerical results and observations, we speculate the following observation (or conjecture) for the FSO in (1.1) with potential:

Conjecture II (Gaps and their distribution statistics of the FSO in (1.1) with potential) Assume $1 < \alpha \le 2$ and $V(x) \in L^{\infty}(\Omega)$ in (1.1), then we have the following asymptotics of its eigenvalues:

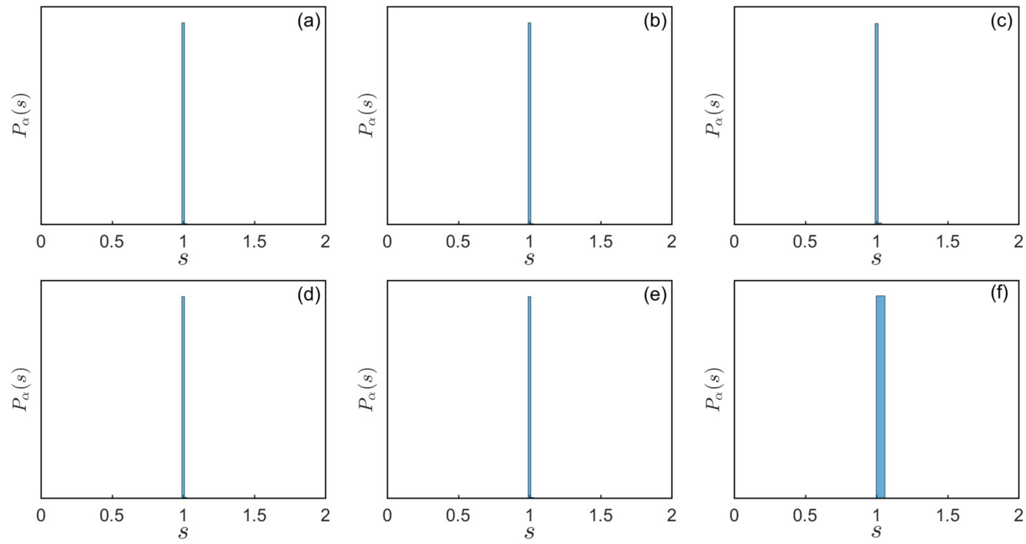

Fig. 14. The histogram of the normalized gaps $\{\delta^{\alpha}_{\text{norm}}(n) \mid 1 \le n \le N = 4096\}$ of (1.1) with $\Omega = (-1, 1)$ and $V(x) = \frac{x^2}{2}$ for different α: (a) $\alpha = 2.0$, (b) $\alpha = 1.9$, (c) $\alpha = \sqrt{3}$, (d) $\alpha = 1.5$, (e) $\alpha = 1.0$, and (f) $\alpha = 0.5$.

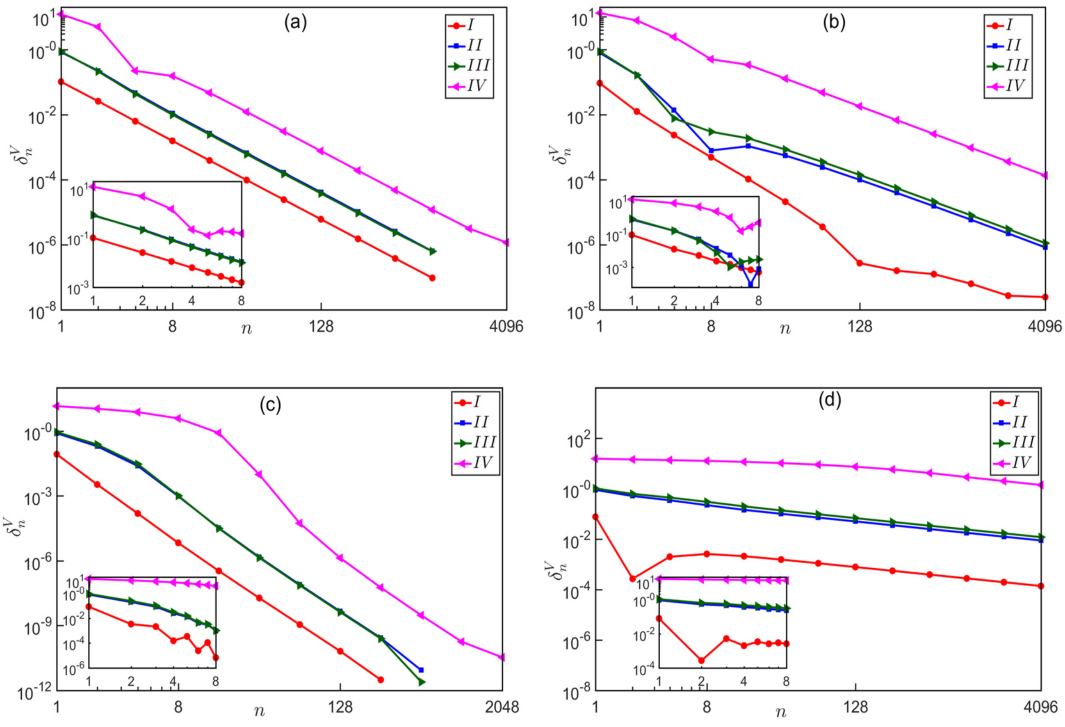

Fig. 15. Differences of the eigenvalues of (1.1) with potential V and without potential, i.e. $\delta_n^V := \lambda_n^\alpha - \lambda_n^{\alpha,0} - C_V$ $(1 \le n \le N = 4096)$ for different potentials $V(x)$ and α: (a) $\alpha = 2$, (b) $\alpha = \sqrt{2}$, (c) $\alpha = 1$, and (d) $\alpha = 0.5$.

$$\lambda_n^\alpha = \begin{cases} \left(\frac{n\pi}{b-a}\right)^\alpha - \left(\frac{\pi}{b-a}\right)^\alpha \frac{\alpha(2-\alpha)}{4} n^{\alpha-1} + C_V + O(n^{\alpha-2}), & 1 < \alpha \le 2, \\ \frac{n\pi}{b-a} - \frac{\pi}{4(b-a)} + C_V + O(n^{-1}), & \alpha = 1, \\ \left(\frac{n\pi}{b-a}\right)^\alpha + C_V - \left(\frac{\pi}{b-a}\right)^\alpha \frac{\alpha(2-\alpha)}{4} n^{\alpha-1} + O(n^{-\alpha}), & 0 < \alpha < 1, \end{cases} \qquad n \gg 1, \tag{5.3}$$

where

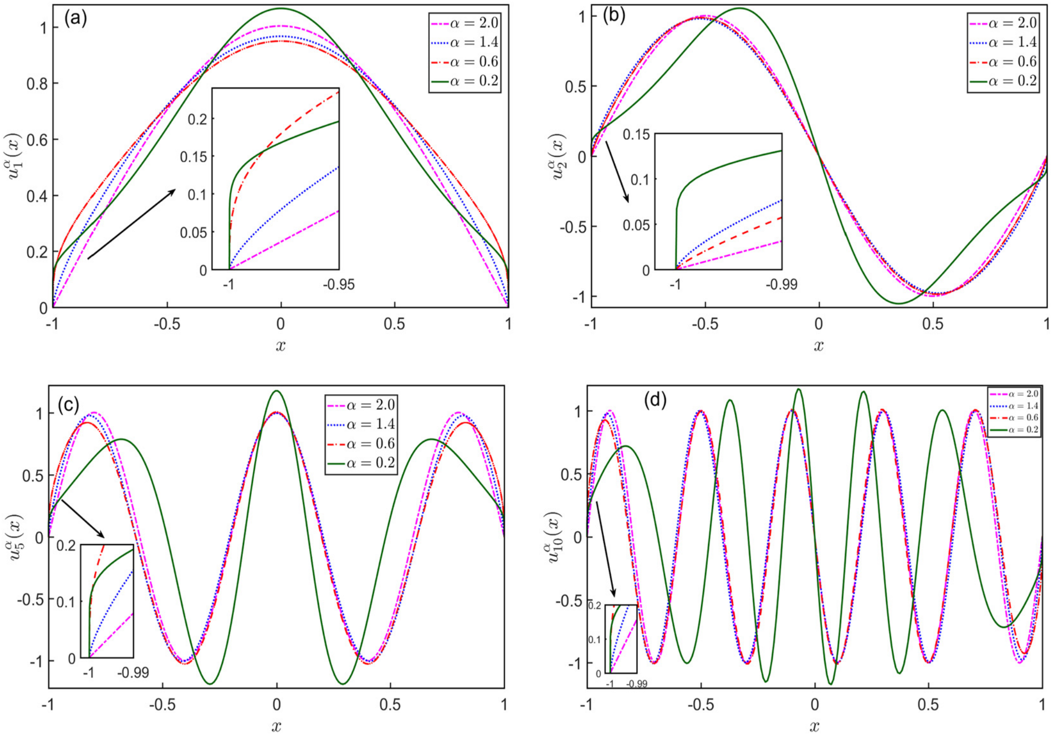

Fig. 16. Plots of different eigenfunctions of (1.1) with $\Omega=(-1,1)$, $V(x)=\frac{x^2}{2}$ and different α: (a) the first eigenfunction $u_1^\alpha(x)$, (b) the second eigenfunction $u_2^\alpha(x)$, (c) the fifth eigenfunction $u_5^\alpha(x)$, and (d) the tenth eigenfunction $u_{10}^\alpha(x)$.

$$C_V=\frac{1}{|\Omega|}\int\limits_{\Omega} V(x)dx=\frac{1}{b-a}\int\limits_a^b V(x)dx. \tag{5.4}$$

In addition, we have the following asymptotics for different gaps:

$$\begin{aligned}
&\delta_{\rm nn}^\alpha(N)\approx\left(\frac{\pi}{b-a}\right)^\alpha\left[\alpha N^{\alpha-1}+\frac{\alpha(\alpha-1)(2+\alpha)}{4}N^{\alpha-2}+O(N^{\alpha-3})\right],\qquad 0<\alpha\le 2,\\
&\delta_{\rm min}^\alpha(N)=\lambda_{N+1}^\alpha-\lambda_N^\alpha\approx\alpha\left(\frac{\pi}{b-a}\right)^\alpha N^{\alpha-1},\qquad 0<\alpha<1,\\
&\delta_{\rm ave}^\alpha(N)\approx\left(\frac{\pi}{b-a}\right)^\alpha\begin{cases}\left[N^{\alpha-1}+\frac{\alpha(2+\alpha)}{4}N^{\alpha-2}+O(N^{-1})\right], & 1<\alpha\le 2,\\ \left[1+\left(\frac{3}{4}-\frac{b-a}{\pi}\lambda_1^{\alpha=1}\right)N^{-1}+O(N^{-2})\right], & \alpha=1,\\ \left[N^{\alpha-1}-\left(\frac{b-a}{\pi}\right)^\alpha\lambda_1^\alpha N^{-1}+O(N^{\alpha-2})\right], & 0<\alpha<1,\end{cases}\qquad N\gg 1.\\
&\delta_{\rm norm}^\alpha(N)\approx 1+O(N^{-2}),\qquad 0<\alpha\le 2,
\end{aligned} \tag{5.5}$$

In addition, for the gaps distribution statistics defined in (1.11), we have

$$P_\alpha(s)=\delta(s-1),\qquad s\ge 0,\qquad 0<\alpha\le 2. \tag{5.6}$$

6. Extension to the directional fractional Schrödinger operator in high dimensions

In this section, we extend the Jacobi spectral method (JSM) presented in Section 2 to the directional fractional Schrödinger operator (D-FSO) in high dimensions and apply it to study numerically its eigenvalues and their gaps as well as gaps distribution statistics.

6.1. The D-FSO in high dimensions

Consider the eigenvalue problem related to the D-FSO in high dimensions:

Find $\lambda \in \mathbb{R}$ and a nonzero real-valued function $u(\mathbf{x}) \neq 0$ such that

$$\begin{aligned} &L_{\text{D-FSO}}\, u(\mathbf{x}) := \left[\mathcal{D}_{\mathbf{x}}^{\alpha} + V(\mathbf{x})\right] u(\mathbf{x}) = \lambda\, u(\mathbf{x}), \qquad \mathbf{x} \in \Omega := (-L_1, L_1) \times \ldots (-L_d, L_d) \subset \mathbb{R}^d, \\ &u(\mathbf{x}) = 0, \qquad \mathbf{x} \in \Omega^c := \mathbb{R}^d \backslash \Omega, \end{aligned} \tag{6.1}$$

where $d \geq 2$, $\mathbf{x} = (x_1, x_2, \ldots, x_d)^T$, $0 < \alpha \leq 2$, $V(\mathbf{x}) \in L^{\infty}(\Omega)$ is a given real-valued function and the directional fractional Laplacian operator $\mathcal{D}_{\mathbf{x}}^{\alpha} := \sum_{j=1}^{d} (-\partial_{x_j x_j})^{\alpha/2}$ is defined via the Fourier transform (see [19,54,46] and references therein) as

$$\mathcal{D}_{\mathbf{x}}^{\alpha}\, u(\mathbf{x}) = \mathcal{F}^{-1}\left(\sum_{j=1}^{d} |\xi_j|^{\alpha} (\mathcal{F}u)(\boldsymbol{\xi})\right), \qquad \mathbf{x}, \boldsymbol{\xi} \in \mathbb{R}^d, \tag{6.2}$$

with $\boldsymbol{\xi} = (\xi_1, \xi_2, \ldots, \xi_d)^T$, $\mathcal{F}$ and $\mathcal{F}^{-1}$ the Fourier transform and the inverse Fourier transform over $\mathbb{R}^d$ [58,64], respectively. We remark here that the directional fractional Laplacian operator $\mathcal{D}_{\mathbf{x}}^{\alpha}$ has been widely used in the literature for different fractional PDEs, see [47,68,52,33,46] and references therein. Again, when $\alpha = 2$, (6.1) collapses to the Schrödinger operator in high dimensions. Specifically, when $\alpha = 2$, $d = 2$ and $L_1 = L_2$ in (6.1), gaps and their distribution of a square billiard can be found in [26,34]. Without loss of generality, we assume that $L_1 \geq L_2 \geq \ldots \geq L_d > 0$.

Again, since all eigenvalues of (6.1) are distinct (or all spectrum are discrete and no continuous spectrum) [5], similar to (1.4) for (1.1), we can also rank (or order) all eigenvalues of (6.1) as (1.4), while again the times that an eigenvalue λ of (6.1) appears in the sequence (1.4) is the same as its algebraic multiplicity. Under the order of all eigenvalues in (1.4) for (6.1), we define the fraction of the repeated eigenvalues of (6.1) as

$$R^{\alpha}(N) := \frac{\#\{2 \leq n \leq N \mid \lambda_n^{\alpha} = \lambda_{n-1}^{\alpha}\}}{N}, \qquad N = 2, 3, \ldots. \tag{6.3}$$

In addition, let $0 < \lambda_1^{\alpha,0} < \lambda_2^{\alpha,0} < \ldots < \lambda_n^{\alpha,0} < \ldots$ be all eigenvalues of (1.1) with $\Omega = (-1, 1)$ and $V(x) \equiv 0$, and $u_n^{\alpha,0}(x)$ $(n = 1, 2, \ldots)$ be the corresponding eigenfunctions. Then when $V(\mathbf{x}) \equiv 0$ in (6.1), all eigenvalues of the problem (6.1) can be given as

$$\lambda_{j_1 \ldots j_d}^{\alpha} = \sum_{l=1}^{d} L_l^{-\alpha} \lambda_{j_l}^{\alpha,0}, \qquad j_1, \ldots, j_d = 1, 2, \ldots, \tag{6.4}$$

and their corresponding eigenfunctions can be given as

$$u_{j_1 \ldots j_d}^{\alpha}(\mathbf{x}) = \Pi_{l=1}^{d} u_{j_l}^{\alpha,0}(x_l/L_l), \qquad \mathbf{x} \in \bar{\Omega}, \qquad j_1, \ldots, j_d = 1, 2, \ldots. \tag{6.5}$$

The above results immediately imply that the fundamental gap of (6.1) with $V(\mathbf{x}) \equiv 0$ can be obtained as

$$\delta_{\text{fg}}(\alpha) = L_1^{-\alpha} \lambda_2^{\alpha,0} + \sum_{l=2}^{d} L_l^{-\alpha} \lambda_1^{\alpha,0} - \sum_{l=1}^{d} L_l^{-\alpha} \lambda_1^{\alpha,0} = L_1^{-\alpha}\left(\lambda_2^{\alpha,0} - \lambda_1^{\alpha,0}\right) \geq \frac{\lambda_2^{\alpha,0} - \lambda_1^{\alpha,0}}{(D/2)^{\alpha}}, \tag{6.6}$$

where D is the diameter of Ω.

The JSM presented in Section 2 can be easily extended to solve the eigenvalue problem (6.1) by tensor product [52]. The details are omitted here for brevity.

6.2. Numerical results in 2D without potential

We take $d = 2$, $L_1 = 1$ and $V(\mathbf{x}) \equiv 0$ in (6.1). In this case, noting (6.4) and (6.5) with $d = 2$, instead of using the JSM in 2D to compute eigenvalues and their corresponding eigenfunctions of (6.1), a simple and more efficient and accurate way is to first use the JSM in 1D to compute the eigenvalues and their corresponding eigenfunctions of (1.1) with $\Omega = (-1, 1)$ and $V(x) \equiv 0$, and then to get the eigenvalues and their corresponding eigenfunctions of (6.1) with $d = 2$ and $V(\mathbf{x}) \equiv 0$ via (6.4) and (6.5) with $d = 2$.

In our computations, we first use the JSM in 1D with $M = 8192$ to compute numerically the eigenvalues of (1.1) with $\Omega = (-1, 1)$ and $V(x) \equiv 0$. Then we use the first $N = 4096$ computed eigenvalues to get the eigenvalues of (6.1) with $d = 2$ and $V(\mathbf{x}) \equiv 0$ via (6.4) with $d = 2$ and then rank (or order) the total 4096×4096 eigenvalues of (6.1) as (1.4). Finally, we take (up to) the first $N = 4000000$ eigenvalues to compute the gaps and their distribution statistics.

Fig. 17 displays the eigenvalues (in increasing order) of (6.1) for different L_2 and α, which suggests that $\lambda_n^{\alpha} \sim n^{\alpha/2}$ when $n \gg 1$ for $0 < \alpha \leq 2$. Then we fit numerically λ_n^{α} when $n \gg 1$ by $C_2^{\alpha} n^{\alpha/2}$. Fig. 18 displays the fitting results of C_2^{α} with respect to the area $S = 4L_2$ of Ω and α, which suggests that

$$C_2^{\alpha} = \frac{4}{2+\alpha}\left(\frac{4\pi}{S}\right)^{\alpha/2}, \qquad 0 < \alpha \leq 2, \qquad S = 4L_2 > 0. \tag{6.7}$$

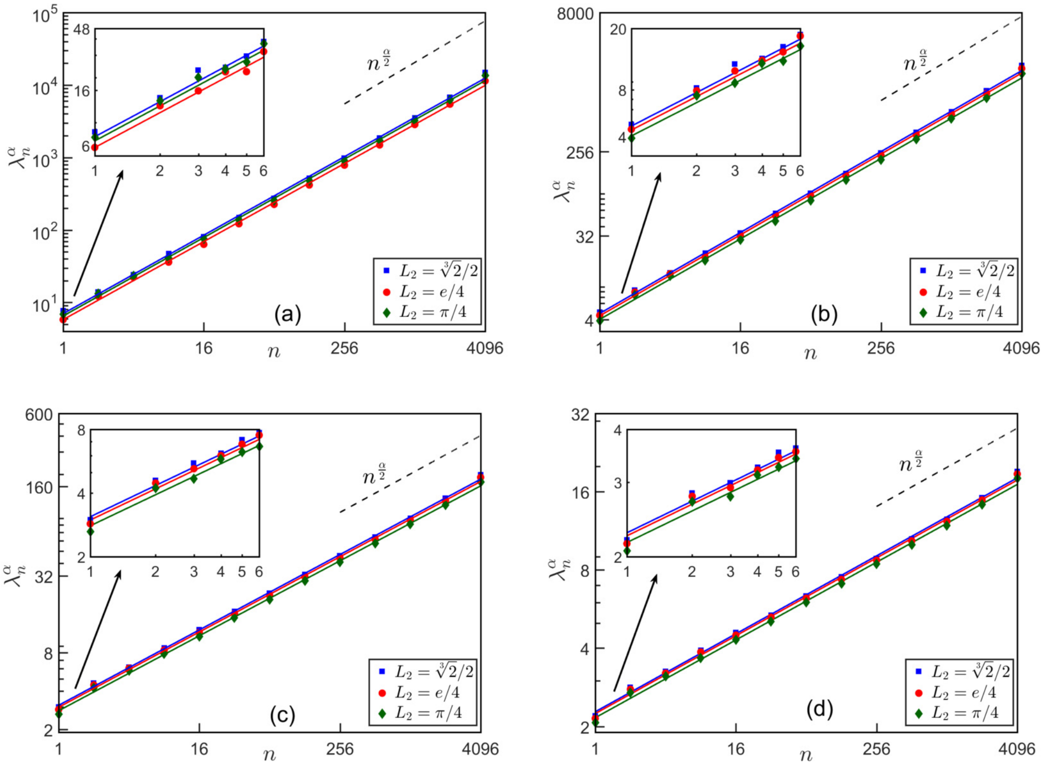

Fig. 17. Eigenvalues of (6.1) with $d = 2$, $L_1 = 1$, $V(\mathbf{x}) \equiv 0$ and different L_2 and α (symbols denote numerical results and solid lines are from the fitting formula $C_2^\alpha n^{\alpha/2}$ when $n \gg 1$): (a) $\alpha = 1.9$, (b) $\alpha = 1.5$, (c) $\alpha = 1.0$, and (d) $\alpha = 0.5$.

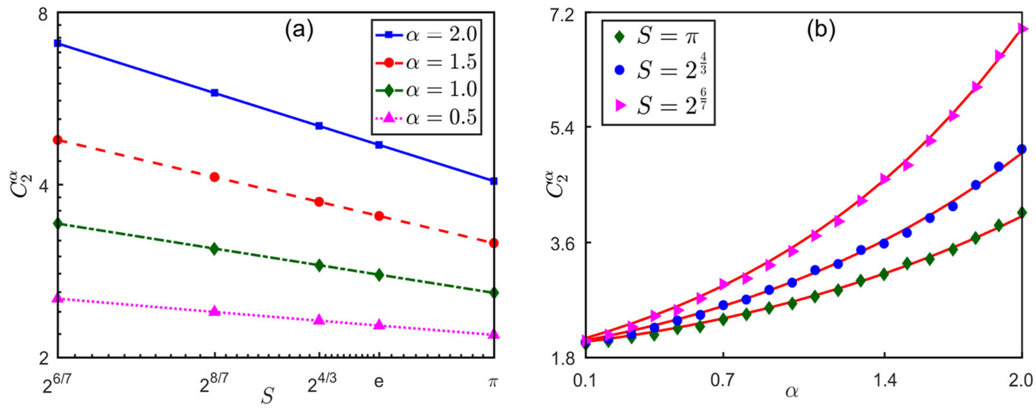

Fig. 18. Numerical results of C_2^α (symbols denote numerical results and solid lines are from the fitting formula (6.7)) for different areas $S = |\Omega| = 4L_2$ and α: (a) plots of C_2^α as a function of S for different α, and (b) plots of C_2^α as a function of α for different S.

These results immediately suggest that

$$\lambda_n^\alpha = \frac{4}{2+\alpha}\left(\frac{4\pi}{S}\right)^{\alpha/2} n^{\alpha/2} + o(n^{\alpha/2}), \qquad n \gg 1. \tag{6.8}$$

Specifically, when $\alpha = 2$, our numerical results suggest that

$$\lambda_n^{\alpha=2} = \frac{4\pi}{S}\left[n + C_1 n^{1/2} + O(1)\right], \qquad n \gg 1, \tag{6.9}$$

where $C_1 \approx 0.5943$ from our numerical results. In fact, (6.9) can be regarded as an improved Weyl law when $\alpha = 2$ [67], and (6.8) can be regarded as an extension of the Weyl law for $\alpha = 2$ [67] to $0 < \alpha \le 2$, and we call (6.8) as the generalized Weyl law on the asymptotics of the eigenvalues of the D-FSO in 2D.

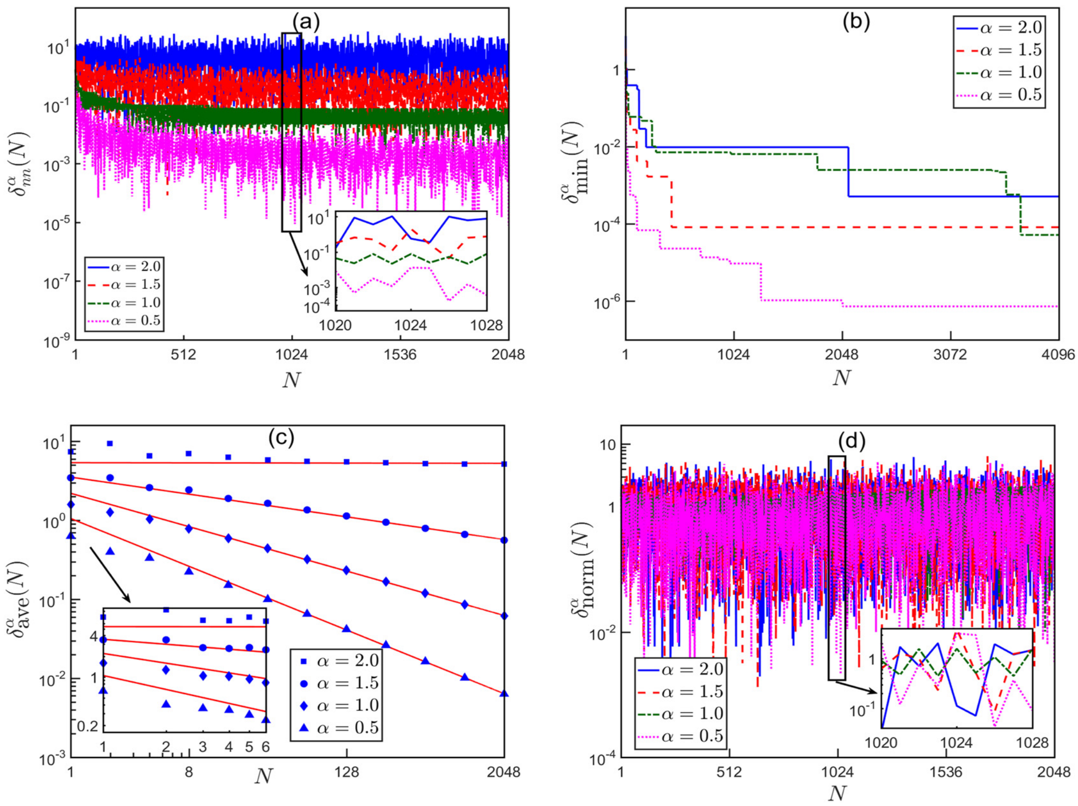

Fig. 19. Different eigenvalue gaps of (6.1) with $d = 2$, $L_1 = 1$, $V(\mathbf{x}) \equiv 0$, $L_2 = \frac{\sqrt[3]{2}}{2}$ and different α for: (a) the nearest neighbour gaps $\delta^{\alpha}_{\text{nn}}(N)$, (b) the minimum gaps $\delta^{\alpha}_{\min}(N)$, (c) the average gaps $\delta^{\alpha}_{\text{ave}}(N)$ (symbols denote numerical results and solid lines are from fitting formulas when $N \gg 1$), and (d) the normalized gaps $\delta^{\alpha}_{\text{norm}}(N)$.

In fact, combining (6.8) and (1.7), we can obtain the asymptotic of the average gaps of the D-FSO in (6.1) as

$$\begin{aligned}
\delta^{\alpha}_{\text{ave}}(N) &= \frac{\lambda^{\alpha}_{N+1} - \lambda^{\alpha}_{1}}{N} \\
&= \frac{1}{N}\left[\frac{4}{2+\alpha}\left(\frac{4\pi}{S}\right)^{\alpha/2} (N+1)^{\alpha/2} + o((N+1)^{\alpha/2}) - \lambda^{\alpha}_{1}\right] \\
&= \frac{4}{2+\alpha}\left(\frac{4\pi}{S}\right)^{\alpha/2} N^{(\alpha-2)/2} + o(N^{(\alpha-2)/2}) \\
&= O(N^{(\alpha-2)/2}), \qquad N \gg 1,
\end{aligned} \tag{6.10}$$

which immediately implies that, when $\alpha = 2$, $\delta^{\alpha}_{\text{ave}}(N) \sim 1$ (i.e. almost a constant) when $N \gg 1$, and respectively, when $0 < \alpha < 2$, $\delta^{\alpha}_{\text{ave}}(N) \sim N^{(\alpha-2)/2}$ (decrease with respect to N) when $N \gg 1$.

In addition, Fig. 19 plots different eigenvalue gaps of (6.1) with $d = 2$, $L_1 = 1$, $V(\mathbf{x}) \equiv 0$, $L_2 = \sqrt[3]{2}/2$ and different α. Fig. 20 displays the histogram of the normalized gaps $\{\delta^{\alpha}_{\text{norm}}(n) \mid 1 \le n \le N = 4000000\}$ for different α and L_2. Fig. 21 plots $1 - R^{\alpha}(N)$ vs N ($N \gg 1$) for different α and L_2.

From Figs. 19–21, we can draw the following conclusions:

(i) The minimum gaps $\delta_{\min}(N) \to 0$ when $N \to +\infty$ (cf. Fig. 19b); and the average gaps $\delta_{\text{ave}}(N) \sim 1$ when $N \gg 1$ for $\alpha = 2$, and respectively, $\delta_{\text{ave}}(N) \sim N^{(\alpha-2)/2}$ when $N \gg 1$ for $0 < \alpha < 2$ (cf. Fig. 19c), which confirm the asymptotic results in (6.10).

(ii) When $L_2 = 1$ and $0 < \alpha \le 2$ or $\alpha = 2$ and $L_2 \in \mathbb{Q}$ or $\alpha = 1$ and $L_2 \in \mathbb{Q}$, the gaps distribution statistics $P_\alpha(s) = \delta(s)$ (cf. Fig. 20a,b,d,g,h,j and Fig. 21). In these cases, $R^{\alpha}(N) \to 1$ when $N \to \infty$ (cf. Fig. 21) and our numerical results suggest the following asymptotics: $R^{\alpha}(N) = 1 - N^{-\tau_2(L_2)}$ when $\alpha = 2$ for different $L_2 \in \mathbb{Q}$ (cf. Fig. 21a); $R^{\alpha}(N) = 1 - N^{-1/2}$ when $\alpha = 1$ for different $L_2 \in \mathbb{Q}$ (cf. Fig. 21b); and $R^{\alpha}(N) = 1 - N^{-\tau_3(\alpha)}$ when $L_2 = 1$ for different $0 < \alpha \le 2$ (cf. Fig. 21c). In addition, Fig. 22 plots $\tau_2(L_2)$ and $\tau_3(\alpha)$ based on our numerical results.

(iii) When $L_2 \notin \mathbb{Q}$ and $0 < \alpha < 1$ or $1 < \alpha \le 2$, $P_\alpha(s)$ can be well approximated by a Poisson distribution (cf. Fig. 20c,e,f,l,m), i.e.

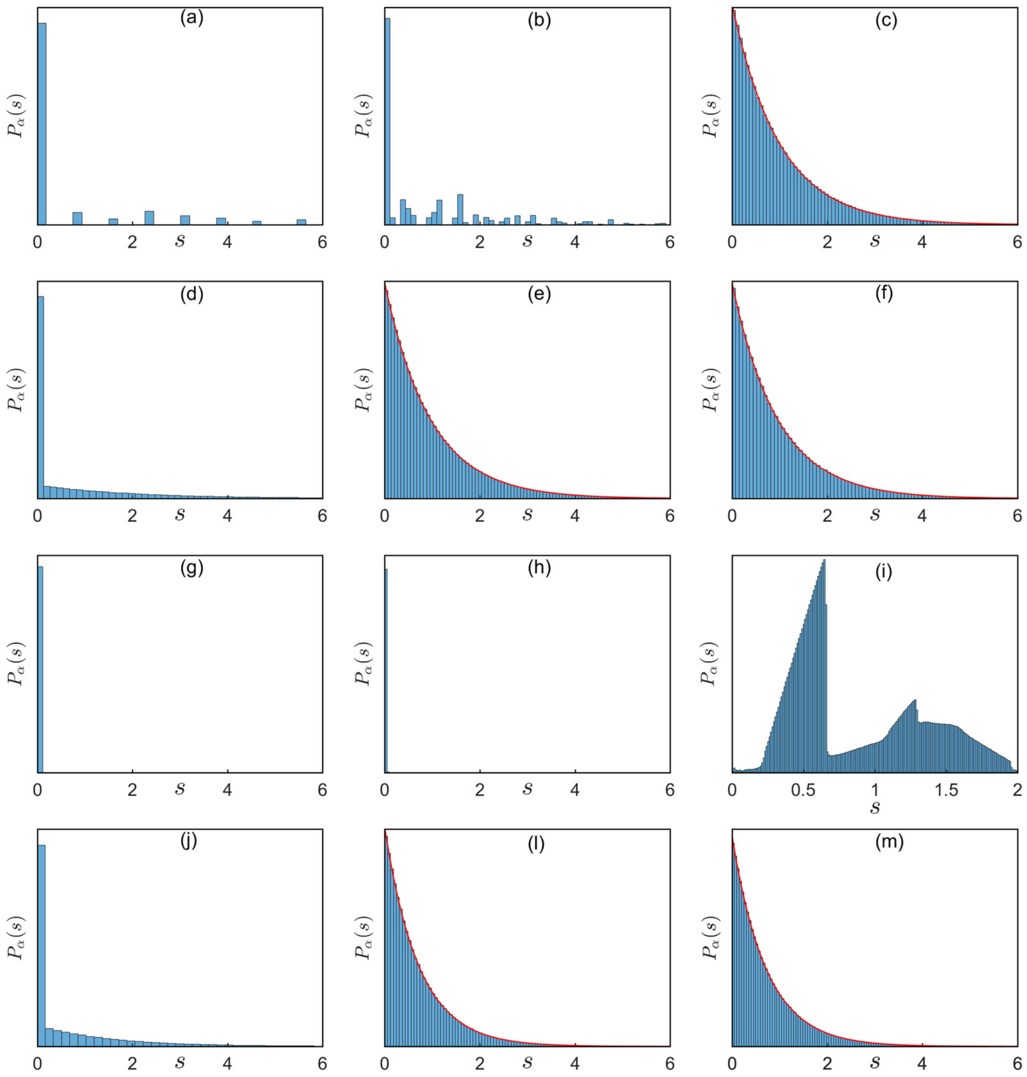

Fig. 20. The histogram of the normalized gaps $\{\delta^{\alpha}_{\mathrm{norm}}(n) \mid 1 \le n \le N = 4000000\}$ of (6.1) with $d = 2$, $L_1 = 1$ and $V(\mathbf{x}) \equiv 0$ for different $0 < \alpha \le 2$ and $0 < L_2 \le 1$: (a) $\alpha = 2.0$ and $L_2 = 1$, (b) $\alpha = 2.0$ and $L_2 = 2/3$, (c) $\alpha = 2.0$ and $L_2 = \frac{\sqrt[3]{2}}{2}$; (d) $\alpha = 1.5$ and $L_2 = 1$, (e) $\alpha = 1.5$ and $L_2 = 2/3$, (f) $\alpha = 1.5$ and $L_2 = \frac{\sqrt[3]{2}}{2}$; (g) $\alpha = 1.0$ and $L_2 = 1$, (h) $\alpha = 1.0$ and $L_2 = 2/3$, (i) $\alpha = 1.0$ and $L_2 = \frac{\sqrt[3]{2}}{2}$; (j) $\alpha = 0.5$ and $L_2 = 1$, (l) $\alpha = 0.5$ and $L_2 = 2/3$, (m) $\alpha = 0.5$ and $L_2 = \frac{\sqrt[3]{2}}{2}$. Solid lines are fitting curves for the gaps distribution statistics $P_\alpha(s)$.

$$P_\alpha(s) = \tau(\alpha) e^{-\tau(\alpha)s}, \qquad s \ge 0. \tag{6.11}$$

In addition, Fig. 23 plots $\tau(\alpha)$, which suggests that

$$\tau(\alpha) \approx \begin{cases} 1, & 1 < \alpha \le 2, \\ 1.057\alpha^{-0.385}, & 0 < \alpha < 1. \end{cases} \tag{6.12}$$

(iv) When $\alpha = 1$ and $L_2 \notin \mathbb{Q}$, $P_\alpha(s)$ can be well approximated by a bimodal distribution [55] (cf. Fig. 20i).

(v) The classification of the gaps distribution statistics $P_\alpha(s)$ for different $0 < \alpha \le 2$ and $L_1 > 0$ and $L_2 > 0$ is summarized in Table 6.

6.3. Numerical results in 2D with potential

Here we use the JSM in 2D to compute numerically the eigenvalues and their corresponding eigenfunctions of (6.1) with $d = 2$ and a non-zero potential $V(x, y)$. In our computations, we choose the total DOF $M = 144 \times 144$, i.e. with DOFs $M_1 = 144$ and $M_2 = 144$ in x_1 and x_2 directions, respectively. With the M eigenvalues computed, we only use $M/4$ (or even less) numerical eigenvalues to compute gaps and their distribution statistics. We take $L_1 = 1$ and $V(x, y) = \frac{x^2+y^2}{2}$ in (6.1).

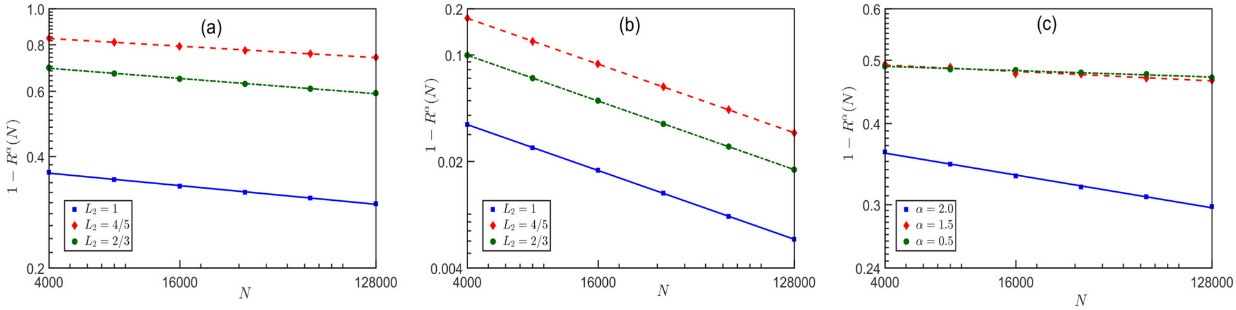

Fig. 21. Plots of $1-R^{\alpha}(N)$ vs N ($N \gg 1$) for different α and L_2: (a) $\alpha=2$ for different $L_2 \in \mathbb{Q}$; (b) $\alpha=1$ for different $L_2 \in \mathbb{Q}$; and (c) $L_2=1$ for different $0<\alpha\le 2$.

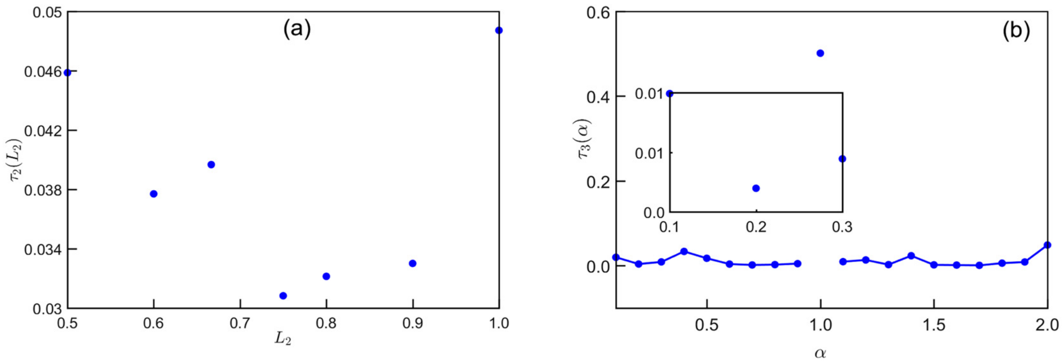

Fig. 22. Fitting results of $\tau_2(L_2)$ for different $L_2 \in \mathbb{Q}$ (left) and $\tau_3(\alpha)$ for different α (right).

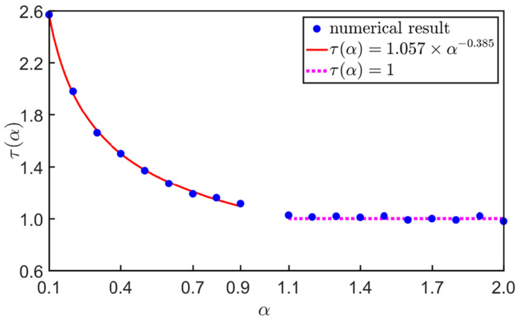

Fig. 23. Fitting results of $\tau(\alpha)$ for different α.

Table 6
Summary of the gaps distribution statistics of (6.1) with $d=2$ and $V(\mathbf{x})\equiv 0$ for different $0<\alpha\le 2$ and $L_1>0$ and $L_2>0$.

	$L_2/L_1=1$	$1\neq L_2/L_1\in\mathbb{Q}$	$1\neq L_2/L_1\notin\mathbb{Q}$
$\alpha=2$	$\delta(s)$	$\delta(s)$	Poisson
$1<\alpha<2$	$\delta(s)$	Poisson	Poisson
$\alpha=1$	$\delta(s)$	$\delta(s)$	Bimodal distribution
$0<\alpha<1$	$\delta(s)$	Poisson	Poisson

Fig. 24 plots different eigenvalue gaps of (6.1) with $L_2=\sqrt[3]{2}/2$ for different α, and Fig. 25 displays the histogram of the normalized gaps $\{\delta^{\alpha}_{\text{norm}}(n) \mid 1\le n\le N=4096\}$ for different α and L_2.

We also carry out numerical simulations on the eigenvalues and their different gaps as well as the gaps distribution statistics of (6.1) in 2D with different other potentials. Our numerical results suggest that the asymptotic behaviour of the eigenvalue λ^{α}_n in (6.8) and (6.9) are still valid when (6.1) is with a potential $V(\mathbf{x})\in L^{\infty}(\Omega)$. In addition, similar to the 1D case, the gaps and their distribution statistics of (6.1) with a potential are quite similar to those without potential, which are reported in Figs. 19&20. Those numerical results are omitted here for brevity.

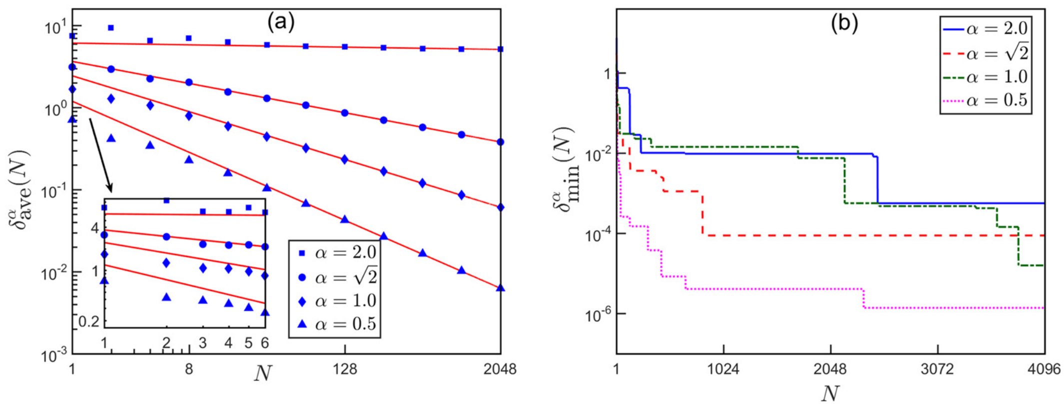

Fig. 24. Different gaps of (6.1) with $d = 2$, $L_1 = 1$, $L_2 = \sqrt[3]{2}/2$ and $V(x, y) = \frac{x^2+y^2}{2}$: (a) the average gaps $\delta^{\alpha}_{\text{ave}}(N)$ (symbols denote numerical results and solid lines are from fitting formulas when $N \gg 1$), and (b) the minimum gaps $\delta^{\alpha}_{\min}(N)$.

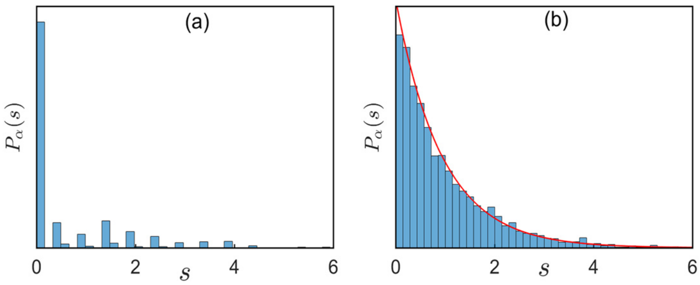

Fig. 25. The histogram of the normalized gaps $\{\delta^{\alpha}_{\text{norm}}(n) \mid 1 \le n \le N = 4096\}$ of (6.1) with $d = 2$ and $V(x, y) = \frac{x^2+y^2}{2}$: (a) $\alpha = 2$ and $L_2 = 1$; and (b) $\alpha = \sqrt{2}$ and $L_2 = \sqrt[3]{2}/2$ (the solid line is a fitting curve by the Poisson distribution).

Finally, based on our extensive numerical results and observations, we speculate the following observation (or conjecture) for the D-FSO in (6.1) without/with potential:

Conjecture III (Gaps and their distribution statistics of the D-FSO in (6.1) in 2D, i.e. $d = 2$) Assume $0 < \alpha \le 2$ and $V(x) \in L^{\infty}(\Omega)$ in (6.1), then we have the following asymptotics of its eigenvalues:

$$\lambda^{\alpha}_n = \frac{4}{2+\alpha}\left(\frac{4\pi}{S}\right)^{\alpha/2} n^{\alpha/2} + o(n^{\alpha/2}), \qquad n \gg 1, \tag{6.13}$$

where S is the area of Ω. In addition, we have the following asymptotics of different gaps:

$$\begin{aligned} &\delta^{\alpha}_{\min}(N) \to 0, \qquad N \to +\infty, \\ &\delta^{\alpha}_{\text{ave}}(N) = \frac{4}{2+\alpha}\left(\frac{4\pi}{S}\right)^{\alpha/2} N^{(\alpha-2)/2} + o(N^{(\alpha-2)/2}), \qquad N \gg 1. \end{aligned} \tag{6.14}$$

Finally the gaps distribution statistics summarized in Table 6 is also valid for (6.1) in 2D with potential $V(\mathbf{x})$.

7. Conclusion

We proposed a Jacobi-Galerkin spectral method for accurately computing a large amount of eigenvalues of the fractional Schrödinger operator (FSO). A very important advantage of the proposed numerical method is that, under a fixed number of degree of freedoms M, the Jacobi spectral method can calculate accurately a large number of eigenvalues with the number proportional to M. Based on the eigenvalues obtained numerically by the proposed method, we obtained several important and interesting results for the eigenvalues and their different gaps of the FSO in 1D and the directional FSO in 2D. Based on the gaps, the distribution statistics of the normalized gaps were obtained numerically for the FSO.

Declaration of competing interest

The authors declare that they have no known competing financial interests or personal relationships that could have appeared to influence the work reported in this paper.

Acknowledgement

The first author thanks very stimulating discussion with Professor Zeev Rudnick. This work was partially support by the Ministry of Education - Singapore grant R-146-000-290-114 (W. Bao), the National Natural Science Foundation of China Grants 11671166 (L.Z. Chen), U1930402 (L.Z. Chen & Y. Ma) and 11771254 (X.Y. Jiang). Part of the work was done when the authors were visiting the Institute for Mathematical Sciences at the National University of Singapore in 2019 (W. Bao and Y. Ma).

References

[1] B. Andrews, J. Clutterbuck, Proof of the fundamental gap conjecture, J. Am. Math. Soc. 24 (2010) 899–916.
[2] X. Antoine, Q.L. Tang, Y. Zhang, On the ground states and dynamics of space fractional nonlinear Schrödinger/Gross-Pitaevskii equations with rotation term and nonlocal nonlinear interactions, J. Comput. Phys. 325 (2016) 74–97.
[3] X. Antoine, E. Lorin, Explicit computation of Robin parameters in optimized Schwarz waveform relaxation methods for Schrödinger equations based on pseudo differential operators, Commun. Comput. Phys. 27 (2020) 1032–1052.
[4] M.S. Ashbaugh, R. Benguria, Optimal lower bound for the gap between the first two eigenvalues of one-dimensional Schrödinger operators with symmetric single-well potentials, Proc. Am. Math. Soc. 105 (1989) 419–424.
[5] I. Babuška, J.E. Osborn, Eigenvalue Problems, Handbook of Numerical Analysis, 1991.
[6] P. Bader, S. Blanes, F. Casas, Solving the Schrödinger eigenvalue problem by the imaginary time propagation technique using splitting methods with complex coefficients, J. Chem. Phys. 139 (2013) 124117.
[7] L. Banjai, J.M. Melenk, R.H. Nochetto, E. Otárola, A.J. Salgado, C. Schwab, Tensor FEM for spectral fractional diffusion, Found. Comput. Math. 19 (2019) 901–962.
[8] W. Bao, N. Ben Abdallah, Y. Cai, Gross-Pitaevskii-Poisson equations for dipolar Bose-Einstein condensate with anisotropic confinement, SIAM J. Math. Anal. 44 (2012) 1713–1741.
[9] W. Bao, X. Dong, Numerical methods for computing ground state and dynamics of nonlinear relativistic Hartree equation for boson stars, J. Comput. Phys. 230 (2011) 5449–5469.
[10] W. Bao, H. Jian, N.J. Mauser, Y. Zhang, Dimension reduction of the Schrödinger equation with Coulomb and anisotropic confining potentials, SIAM J. Appl. Math. 73 (2013) 2100–2123.
[11] W. Bao, X. Ruan, Fundamental gaps of the Gross-Pitaevskii equation with repulsive interaction, Asymptot. Anal. 110 (2018) 53–82.
[12] W. Bao, X. Ruan, J. Shen, C. Sheng, Fundamental gaps of the fractional Schrödinger operator, Commun. Math. Sci. 17 (2019) 447–471.
[13] M.V.D. Berg, On condensation in the free-boson gas and the spectrum of the Laplacian, J. Stat. Phys. 31 (1983) 623–637.
[14] C. Bernardi, Y. Maday, Spectral methods, Handb. Numer. Anal. 5 (1997) 209–485.
[15] D. Boffi, Finite element approximation of eigenvalue problems, Acta Numer. 19 (2010) 1–120.
[16] A. Bonito, J.P. Borthagaray, R.H. Ricardo, E. Otárola, A.J. Abner, Fundamental gaps of the fractional Schrödinger operator, Comput. Vis. Sci. 19 (2018) 19–46.
[17] J.P. Borthagaray, L.M.D. Pezzo, S. Martínez, Finite element approximation for the fractional eigenvalue problem, J. Sci. Comput. 77 (2018) 308–329.
[18] J. Bourgain, V. Blomerand, Z. Rudnick, Small gaps in the spectrum of the rectangular billiard, Ann. Sci. Éc. Norm. Supér. 50 (2017) 1283–1300.
[19] L. Caffarelli, L. Silvestre, An extension problem related to the fractional Laplacian, Commun. Partial Differ. Equ. 32 (2007) 1245–1260.
[20] Y. Cai, M. Rosenkranz, Z. Lei, W. Bao, Mean-field regime of trapped dipolar Bose-Einstein condensates in one and two dimensions, Phys. Rev. A 82 (2010) 043623.
[21] L. Carusotto, C. Citui, Quantum fluids of lights, Rev. Mod. Phys. 85 (2013) 299.
[22] C. Çelik, M. Duman, Crank-Nicolson method for the fractional diffusion equation with the Riesz fractional derivative, J. Comput. Phys. 231 (2012) 1743–1750.
[23] S.L. Chang, C.S. Chien, B.W. Jeng, An efficient algorithm for the Schrödinger-Poisson eigenvalue problem, J. Comput. Appl. Math. 205 (2007) 509–532.
[24] L.Z. Chen, Z.P. Mao, H.Y. Li, Jacobi-Galerkin spectral method for eigenvalue problems of Riesz fractional differential equations, arXiv:1803.03556.
[25] Z.Q. Chen, R. Song, Two sided eigenvalue estimates for subordinate processes in domains, J. Funct. Anal. 226 (2005) 90–113.
[26] R.D. Connors, J.P. Keating, Two-point spectral correlations for the square billiard, J. Phys. A 30 (1997) 1817–1830.
[27] S. Costiner, S. Ta'asan, Simultaneous multigrid techniques for nonlinear eigenvalue problems: solutions of the nonlinear Schrödinger-Poisson eigenvalue problem in two and three dimensions, Phys. Rev. E 52 (1995) 1181.
[28] M. D'Elia, M. Gunzburger, The fractional Laplacian operator on bounded domains as a special case of the nonlocal diffusion operator, Comput. Math. Appl. 66 (2013) 1245–1260.
[29] Q. Du, M. Gunzburger, R.B. Lehoucq, K. Zhou, Ana'lysis and approximation of nonlocal diffusion problems with volume constraints, SIAM Rev. 54 (2012) 667–696.
[30] S.W. Duo, Y.Z. Zhang, Computing the ground and first excited states of the fractional Schrödinger equation in an infinite potential well, Commun. Comput. Phys. 18 (2015) 321–350.
[31] B. Dyda, Fractional calculus for power functions and eigenvalues of the fractional Laplacian, Fract. Calc. Appl. Anal. 15 (2012) 536–555.
[32] A. Elgart, B. Schlein, Mean field dynamics of boson stars, Commun. Pure Appl. Math. 60 (2007) 500–545.
[33] W.P. Fan, F.W. Liu, X.Y. Jiang, I. Tumer, A novel unstructured mesh finite element method for solving the time-space fractional wave equation on a two-dimensional irregular convex domain, Fract. Calc. Appl. Anal. 20 (2017) 352–383.
[34] T. Freiberg, P. Kurlberg, L. Rosenzweig, Poisson distribution for gaps between sums of two squares and level spacings for toral point scatterers, Commun. Number Theory Phys. 11 (2017) 837–877.
[35] P. Grisvard, Elliptic Problems in Nonsmooth Domains, Pitman Advanced Pub, Boston, 1985.
[36] G. Grubb, Fractional Laplacians on domains, a development of Hörmander's theory of μ-transmission pseudodifferential operators, Adv. Math. 268 (2015) 478–528.
[37] G. Grubb, Singular Green operators and their spectral asymptotics, Duke Math. J. 51 (1984) 477–528.
[38] E.M. Harrell, Commutators, eigenvalue gaps, and mean curvature in the theory of Schrödinger operators, Commun. Partial Differ. Equ. 32 (2007) 401–413.
[39] D. Jakobson, S. Miller, I. Rivin, Z. Rudnick, Level spacings for regular graphs, IMA Math. Appl. 109 (1999) 317–329.
[40] S. Jiang, L. Greengard, W. Bao, Fast and accurate evaluation of nonlocal Coulomb and dipole-dipole interactions via the nonuniform FFT, SIAM J. Sci. Comput. 36 (2014) B777–B794.
[41] B.T. Jin, R. Lazarov, J. Pasciak, W. Rundell, A finite element method for the fractional Sturm-Liouville problem, arXiv:1307.5114.
[42] M. Kwaśnicki, Ten equivalent definitions of the fractional Laplace operator, Fract. Calc. Appl. Anal. 20 (2017) 7–51.

[43] M. Kwaśnicki, Eigenvalues of the fractional Laplace operator in the interval, J. Funct. Anal. 262 (2012) 2379–2402.
[44] P. Li, S.T. Yau, On the Schrödinger equation and the eigenvalue problem, Commun. Math. Phys. 88 (1983) 309–318.
[45] J.L. Lions, E. Magenes, Non-homogeneous Boundary Value Problems and Applications, Springer-Verlag, 1972.
[46] A. Lischke, G.F. Pang, M. Gulian, F.Y. Song, C. Glusa, X.N. Zheng, Z.P. Mao, W. Cai, M.M. Meerschaert, M. Ainsworth, What is the fractional Laplacian?, arXiv:1801.09767.
[47] F.W. Liu, S.P. Chen, I. Turner, K. Burrage, V. Anh, Numerical simulation for two-dimensional Riesz space fractional diffusion equations with a nonlinear reaction term, Cent. Eur. J. Phys. 11 (2013) 1221–1232.
[48] O.E. Livne, A. Brandt, Multiscale Eigenbasis Calculations: *N* Eigenfunctions in O(N log N), Springer, Berlin, Heidelberg, 2002.
[49] Y. Luchko, Fractional Schrödinger equation for a particle moving in a potential well, J. Math. Phys. 54 (2013) 012111.
[50] Y. Ma, L. Chen, A Jacobi-Galerkin spectral method for computing the ground and first excited states of nonlinear fractional Schrödinger equation, East Asian J. Appl. Math. 10 (2020) 274–294.
[51] Z.P. Mao, S. Chen, J. Shen, Efficient and accurate spectral method using generalized Jacobi functions for solving Riesz fractional differential equations, Appl. Numer. Math. 106 (2016) 165–181.
[52] Z.P. Mao, J. Shen, Efficient spectral-Galerkin methods for fractional partial differential equations with variable coefficients, J. Comput. Phys. 307 (2016) 243–261.
[53] C. Mehl, S. Borm, Numerical Methods for Eigenvalue Problems, 2008.
[54] E. Di Nezza, G. Palatucci, E. Valdinoci, Hitchhiker's guide to the fractional Sobolev spaces, Bull. Sci. Math. 136 (2012) 521–573.
[55] S. Offermanns, W. Rosenthal, Bimodal Distribution, Springer, Berlin, Heidelberg, 2008.
[56] K.M. Owolabi, A. Atangana, Numerical solution of fractional-in-space nonlinear Schrödinger equation with the Riesz fractional derivative, Eur. Phys. J. Plus 131 (2016) 335.
[57] F. Pinsker, W. Bao, Y. Zhang, H. Ohadi, A. Dreismann, J.J. Baumberg, Fractional quantum mechanics in polariton condensates with velocity dependent mass, Phys. Rev. B 92 (2015) 195310.
[58] I. Podlubny, Fractional Differential Equations, Academic Press, San Diego, 1999.
[59] A. Quarteroni, A. Valli, Numerical Approximation of Partial Differential Equations, Springer, Berlin, Heidelberg, 1994.
[60] S.Y. Reutskiy, A new numerical method for solving high-order fractional eigenvalue problems, J. Comput. Appl. Math. 317 (2017) 603–623.
[61] Z. Rudnick, A metric theory of minimal gaps, Numer. Algorithms 64 (2018) 628–636.
[62] Z. Rudnick, A. Zaharescu, The distribution of spacings between fractional parts of lacunary sequences, Forum Math. 14 (2002) 691–712.
[63] S.G. Samko, A.A. Kilbas, O.I. Marichev, Fractional Integrals and Derivatives, Gordon and Breach Science Publishers, Yverdon, 1993.
[64] J. Shen, T. Tang, L.L. Wang, Spectral Methods: Algorithms, Analysis and Applications, Springer Publishing Company, 2011.
[65] E. Valdinoci, From the long jump random walk to the fractional Laplacian, Bol. Soc. Esp. Mat. Apl. SeMA 49 (2009) 33–44.
[66] J.A.C. Weideman, L.N. Trefethen, The eigenvalues of second-order spectral differentiation matrices, SIAM J. Numer. Anal. 25 (1988) 1279–1298.
[67] H. Weyl, Das asymptotische Verteilungsgesetz der Eigenwerte linearer partieller Differentialgleichungen, Math. Ann. 71 (1912) 441–479.
[68] F. Zeng, F. Liu, C. Li, K. Burrage, I. Turner, V. Anh, A Crank–Nicolson ADI spectral method for a two-dimensional Riesz space fractional nonlinear reaction-diffusion equation, SIAM J. Numer. Anal. 52 (2014) 2599–2622.
[69] X. Zhao, Z. Sun, H.Z. Peng, A fourth-order compact ADI scheme for two-dimensional nonlinear space fractional Schrödinger equation, SIAM J. Sci. Comput. 36 (2014) A2865–A2886.
[70] J.W. Zhang, D.F. Li, X. Antoine, Efficient numerical computation of time-fractional nonlinear Schrödinger equations in unbounded domain, Commun. Comput. Phys. 25 (2019) 218–243.
[71] A. Zoia, A. Rosso, M. Kardar, Fractional Laplacian in bounded domains, Phys. Rev. E 76 (2007) 021116.